

A GLOBAL INVENTORY OF BURNED AREAS AT 1 KM RESOLUTION FOR THE YEAR 2000 DERIVED FROM SPOT VEGETATION DATA

KEVIN TANSEY^{1,*}, JEAN-MARIE GRÉGOIRE², ELISABETTA BINAGHI³,
LUIGI BOSCHETTI², PIETRO ALESSANDRO BRIVIO⁴, DMITRY ERSHOV⁵,
STÉPHANE FLASSE⁶, ROBERT FRASER⁷, DEAN GRAETZ⁸, MARTA MAGGI²,
PASCAL PEDUZZI⁹, JOSÉ PEREIRA^{10,11}, JOÃO SILVA¹¹, ADÉLIA SOUSA¹²
and DANIELA STROPPIANA⁴

¹*Department of Geography, University of Leicester, University Road, Leicester, LE1 7RH, U.K.
E-mail: kevin.tansey@le.ac.uk*

²*European Commission Joint Research Centre (JRC), Ispra (VA), I-21020, Italy*

³*Università dell'Insubria, Via Ravasi 2, I-21100, Varese, Italy*

⁴*Institute for Electromagnetic Sensing of the Environment (CNR-IREA), Via Bassini 15, I-20133,
Milan, Italy*

⁵*International Forest Institute (IFI), Novocheriomushkinskaya str. 69a, Moscow, 117418, Russia*

⁶*Flasse Consulting, 3 Sycamore Crescent, Maidstone, ME16 0AG, U.K.*

⁷*Natural Resources Canada, Canada Centre for Remote Sensing (CCRS), 588 Booth St., Ottawa,
ON, K1A 0Y7, Canada*

⁸*CSIRO Earth Observation Centre GPO 3023, Canberra, ACT, 2601, Australia*

⁹*United Nations Environment Programme – Early Warning Unit (UNEP/DEWA/GRID-Geneva),
International Environment House, 1219 Geneva, Switzerland*

¹⁰*Tropical Research Institute, Travessa Conde da Ribeira 9, 1300-142 Lisbon, Portugal*

¹¹*Department of Forestry, Technical University of Lisbon, Tapada da Ajuda, 1349-017 Lisbon,
Portugal*

¹²*Department of Rural Engineering, University of Évora, Apartado 94, 7002-554 Évora, Portugal*

Abstract. Biomass burning constitutes a major contribution to global emissions of carbon dioxide, carbon monoxide, methane, greenhouse gases and aerosols. Furthermore, biomass burning has an impact on health, transport, the environment and land use. Vegetation fires are certainly not recent phenomena and the impacts are not always negative. However, evidence suggests that fires are becoming more frequent and there is a large increase in the number of fires being set by humans for a variety of reasons. Knowledge of the interactions and feedbacks between biomass burning, climate and carbon cycling is needed to help the prediction of climate change scenarios. To obtain this knowledge, the scientific community requires, in the first instance, information on the spatial and temporal distribution of biomass burning at the global scale. This paper presents an inventory of burned areas at monthly time periods for the year 2000 at a resolution of 1 kilometer (km) and is available to the scientific community at no cost. The burned area products have been derived from a single source of satellite-derived images, the SPOT VEGETATION S1 1 km product, using algorithms developed and calibrated at regional scales by a network of partners. In this paper, estimates of burned area, number of burn scars and average size of the burn scar are described for each month of the year 2000. The information is reported at the country level. This paper makes a significant contribution to understanding the effect of biomass burning on atmospheric chemistry and the storage and cycling of carbon by constraining one of the main parameters used in the calculation of gas emissions.



1. Introduction

Biomass burning is an important driver for global change due to its effect on atmospheric composition and chemistry, climate, biogeochemical cycling of nitrogen and carbon, the hydrological cycle, reflectivity and emissivity of land, and stability of ecosystems (Levine, 1996). Biomass burning is an annual phenomenon affecting almost every vegetated ecosystem on the Earth. In a warming climate, any changes in fire severity or in fire return interval can have major impacts on carbon sequestration and forest health and sustainability (Kasischke et al., 1995). To fully understand the impact of vegetation fires on carbon storage and release, ecosystem functioning and cycling and land management information, the timing and spatial distribution of burning activity is required at the global scale (Malingreau and Grégoire, 1996; Dwyer et al., 1999; Van Aardenne et al., 2001; Andreae and Merlet, 2001). In fact, the area consumed by fire at regional or global scales is one of the parameters that provides the greatest uncertainty in calculating the amount of consumed biomass and emitted gases at this scale (Levine, 1996; Scholes et al., 1996; Barbosa et al., 1999b; Andreae and Merlet, 2001; Isaev et al., 2002), and often burned areas are estimated from ancillary information, indirect methods (i.e. from active fires or gas concentrations) or extrapolated (Pereira et al., 1999; Wotawa et al., 2001; Conard et al., 2002; Schultz, 2002). This paper describes a global inventory of burned areas at a resolution of 1 kilometer (km). The inventory, available in monthly time periods, was derived from satellite data acquired on a daily basis during the year 2000 and processed using fully documented procedures under the Global Burnt Area, 2000 (GBA, 2000) initiative (Tansey, 2002). The impact of burning activity on the global carbon cycle and the interchange of carbon in various forms is complex. Houghton (1991) outlines the role of biomass burning from the perspective of the global carbon cycle. The net contribution of biomass burning to atmospheric CO₂, calculated over the (biologically sensible) annual cycle, is determined by the nature of the fuel (vegetation) consumed. For stand-replacing forest fires where the burned biomass may take decades to centuries to re-grow, or where fire is used to convert land cover types, such as forest to cropland, such that the pre-fire carbon pool of the forest becomes permanently transferred to the atmosphere.

This paper describes an inventory that makes a large leap forward in establishing the timing and location of burning activity at the global scale. The estimates of burned areas in this paper have the distinct advantage in that they are produced from a single source of information, namely satellite data from the VEGETATION (VGT) sensor aboard the European SPOT-4 satellite, and have been derived using common processing routines and algorithms that are well documented. Furthermore, we have a complete global coverage of the land surface on a daily basis from a single image source. This scenario is different to the approach taken by Van der Werf et al. (2004) who used multiple satellite data sources to derive burnt areas at continental scales to determine emissions. Previous estimates of burned areas at the global scale have been derived from compilations of regional scale studies and a best

guess made of remote regions or those not specified in the literature. In addition, estimates often come from many different sources, use complicated methods or are badly documented. Barbosa et al. (1999b) performed an eight-year analysis of burned areas, burned biomass and atmospheric emissions in sub-Saharan Africa, using satellite imagery. They estimated a mean annual burned area between 3.5 and 6.3 million km², during the period 1985–1991. These figures reveal not only the enormous extent of the area affected by fire in Africa but also the wide margin of uncertainty in the estimates. Large variations in published values make the user communities reluctant to utilise the data available to them. This paper reports burnt area estimates that are produced using fully documented algorithms (Tansey, 2002) and while no direct comparisons are made with other estimates, the paper is nonetheless timely and worthwhile. A detailed comparison of burnt area estimates (comparing national statistics, other satellite data products and GBA, 2000) in major vegetation types is given in Tansey et al. (2004).

This paper first describes the satellite data (Section 2) and the methodology (Section 3) used to extract the burned area information. Section 4 provides a detailed documentation and discussion of the burned area distribution (in space and time) in each region of the globe and concludes with validation and accuracy issues.

2. The Satellite-Derived Dataset

Burned area mapping at a regional scale has been performed using the MODIS satellite in southern Africa (Roy et al., 2002) and the Advanced Very High Resolution Radiometer (AVHRR) imagery in tropical savanna (Scholes et al., 1996), boreal forest (Cahoon et al., 1994; Fraser et al., 2000) and Mediterranean forest ecosystems (Fernández et al., 1997; Pereira, 1999). At a continental scale, Barbosa et al. (1999a) developed an algorithm for AVHRR Global Area Coverage (GAC) images over Africa at a resolution of 5 km on a weekly basis. A similar dataset is provided by the ERS Along-Track Scanning Radiometer (ATSR and ATSR-2) systems. These data were used by Eva et al. (1998) to map burnt areas in tropical woodland savanna in Central Africa with some success. In a similar initiative to GBA, 2000, ATSR-2 has been used with some success to map burned areas at the global scale for the year 2000 (Kempeneers et al., 2002). The project, entitled GLOBSCAR and initiated by the European Space Agency (ESA), used the results of two algorithms both applied globally to derive the burned area products. The GLOBSCAR products, available at the same resolution as the GBA, 2000 products, is a valuable dataset for comparison studies (<http://www.geosuccess.net>). Comparisons between GLOBSCAR and GBA, 2000 results are given in Tansey et al. (2004).

The VGT sensor was launched on board the European SPOT 4 platform in March 1998 (<http://www.spot-vegetation.com>). Compared to other instruments offering 1 km products that have been used for burnt area mapping, such as AVHRR and ATSR, the VGT system offers certain advantages. The geometry ensures a high accuracy in

multi-spectral registration (better than 0.2 km), multi-temporal registration (better than 0.5 km) and absolute geolocation (better than 0.8 km). The sensor acquires data in four spectral bands covering the visible (0.43–0.47 μm corresponding to blue wavelengths; 0.61–0.68 μm corresponding to red wavelengths) and near infrared domains (0.78–0.89 μm corresponding to near infrared wavelengths; 1.58–1.75 μm corresponding to short-wave infrared wavelengths). The 2200 km swath width allows imaging over large areas providing daily coverage apart from within the tropics in which 90% of the area is imaged each day and the gap acquired the following day. The acquisition time is 10.30 AM local solar time (descending node). The short-wave infrared band centered at 1.65 μm was shown by Eastwood et al. (1998) to be useful for burnt area mapping. Trigg and Flasse (2000) showed, using *in situ* measurements, the relevance of VGT spectral bands to detect burned areas. The VGT time series used in this work was the daily surface reflectance (S1 product) starting from the December 1, 1999 to December 31, 2000. Global VGT data have been acquired from 1999 and it is the intention of the European Space Agency to process this data and provide multi-annual burnt area data (through the GlobCarbon project).

3. Implementation Strategy of the Burned Area Algorithms

The methods required to detect a burnt area differs from one ecosystem or climatic zone to another (e.g. boreal forest, tropical forest, grasslands). Because of this, the approach taken was to develop regional algorithms, using temporal and spatial subsets of VGT data that corresponded to each project partner's specific region of interest and expertise. The main specifications of these algorithms are described in Table I. Seven algorithms were selected for processing the entire year 2000 dataset and integrated into a global processing chain (Tansey, 2002). The global dataset was distributed into sections depending on large-scale vegetation features or seasonal burning activity. The selection of a suitable algorithm for operational implementation outside regions of algorithm calibration described in Table I was made after looking at different criteria. The first criterion was to look at the main types, distribution and patterns of vegetation in the region (needleleaf forest, broadleaf forest, grasslands etc.) using a global land cover map and select an algorithm that has been developed and successfully applied over a region with similar characteristics. A second criterion was to apply two or three different algorithms to the same area, see how they compared between themselves and also compared to other sources of burned area or active fire information. A third criteria depended on certain characteristics of the region of interest such as topography, presence of agricultural areas, areas tending to flood and urban areas that can all have an influence on the algorithm's results. In a number of regions, it was necessary to use two algorithms to fully capture all of the burning activity. This necessity was driven by evidence of burning activity in daily images (smoke or active fires observed) or through using

TABLE I

Algorithm name	Main characteristics of the algorithm	Region of development	Institute/country	Reference
IFI	Removal of contaminated ¹ pixels, daily values of the NIR ² band are observed for abrupt changes when compared with an intermediate product and other tests are satisfied.	Two regions of Russia: A: 68–60°N; 45–60°E B: 60–48°N; 118–140°E	International Forest Institute (IFI), Moscow, Russia	Ershov and Novik (2001)
UTL (UTL – Africa 1) (UTL – Africa 2) (UTL – Europe) (UTL – Asia)	Removal of contaminated ¹ pixels and composited over a monthly time period using the minimum NIR ² value. Africa 2 uses CART ³ theory to derive decision rules. The other algorithms use Fisher's Linear Discriminant Analysis ⁴ approaches but use different thresholds.	Four regions were provided: Africa 1: 10–28°S; 22–42°E Africa 2: 18°N–35°S; 20°W–55°E Europe: 44–35.5°N; 10°W–0° Asia: 55–40°N; 115–135°E	Technical University of Lisbon (UTL), Portugal (in collaboration with the Tropical Research Institute (TRI), Lisbon, Portugal)	Silva et al. (2002), Silva et al. (2003)
CCRS	Ten-day composites are derived with a max. NDVI ² criteria. A multiple logistic regression model based on ten-day changes, an ecosystem mask and monthly satellite-derived metrics is used. The products are filtered and region grown.	One region of Canada: 62.5–57°N; 112–104.5°W (SPOT VGT S10 ⁵ data from the year 1998 were also used)	Natural Resources Canada, Canadian Centre for Remote Sensing (CCRS), Ottawa, Canada	Fraser et al. (2003)

(Continued on next page)

TABLE I
(Continued)

Algorithm name	Main characteristics of the algorithm	Region of development	Institute/country	Reference
UOE/UTL	Removal of contaminated ¹ pixels and composited over a month using the 3rd min. NIR ² value. The algorithm uses CART ³ theory to derive decision rules from training sets.	One region of Brazil: 5°N–20°S; 75–45°W	University of Evora, Portugal; UTL, Portugal; TRI, Portugal	Silva et al. (2002)
GVM (developed by Stroppiana)	Removal of contaminated ¹ pixels and composited over a ten-day time period using the minimum NIR ² value. The algorithm uses CART ³ theory to derive decision rules from training sets. The resulting products are filtered and summed to create monthly products.	One region of Australia: 11–21°S; 125–135°E	EC Joint Research Centre (JRC), Ispra (VA), Italy	Stroppiana et al. (2002) Stroppiana et al. (2003)
NRI	A change detection algorithm using pre- and post-burn data in the NIR ² and SWIR ² bands. The pre-burn image is updated daily with non-contaminated pixels. To reduce the variation of the spectral signal caused by viewing geometry the algorithm utilises daily data in five-day cycles.	One region of southeast Africa: 17–29°S; 11–30°E	Natural Resources Institute (NRI), University of Greenwich, UK	Boschetti et al. (2002)

CNR	Contextual supervised classification methodology based on hierarchical use of the Multi-Layer Perceptron (MLP) neural network which use the spatial and temporal information of daily images to produce daily maps of burnt areas.	One region of Africa: Africa: 18°N–0°S; 20°W–55°E	CNR—Institute for Electromagnetic Sensing of the Environment (IREA), Milan, Italy	Brivio et al. (2002)
GVM (developed by Boschetti)	Removal of contaminated ¹ pixels and a BRDF ⁶ model is inverted to yield reflectance. A change detection method ⁶ is used to compare values predicted from the model and observed in the NIR ² and SWIR ² bands.	Two regions of Central America: 22–7°N; 93–77°W 33–15°N; 117–93°W	JRC, Ispra (VA), Italy	Boschetti (personal communication), Tansey (2002)

The main characteristics of the burned area algorithms used to derive the global inventory are presented. Further details are presented in Tansey (2002):
¹Contaminated pixels are those of cloud or smoke, cloud shadow, acquired at extreme angles, sensor saturation in the SWIR² band, non-vegetated or in topographic shadow.

²NIR refers to the near infrared band, SWIR refers to the short-wave infrared band. NDVI refers to the normalized difference vegetation index.

³CART is an acronym for Classification Trees and Regression Trees and is described by Breiman et al. (1984).

⁴Fisher's Linear Discriminant Analysis method is described in Johnson and Wichern (1988).

⁵SPOT VGT S10 data refers to products that have been composited over a ten-day period following a maximum NDVI criteria.

⁶BRDF refers to the bi-directional reflectance distribution function. The BRDF model is described by Roujean et al. (1992). The method is adapted from Roy et al. (2002).

higher resolution images such as from Landsat TM quick-looks available freely through the Internet (<http://Glovis.usgs.gov/BrowseBrowser.shtml>). Tansey (2002) provides a complete overview of the spatial and temporal application of the GBA algorithms that is summarized in the next three paragraphs.

The CCRS algorithm was used to derive burned area products for forested regions of Canada and the United States (US) (according to a forest cover map provided by CCRS). The non-forested regions of the US were processed using the first algorithm developed by the UTL group (UTL Africa 1). Southern regions of the US and Central America are processed with the IFI and GVM (developed by Boschetti) algorithms. A window covering the northern half of the South American continent (including the Amazon Forest) was processed with a dedicated algorithm developed by UOE/UTL. The southern half of South America (including Argentina and Chile) was processed solely using the IFI algorithm. After a long period of testing with several algorithms, a single algorithm (UTL Africa 2) was used to derive the burned area products for sub-Saharan Africa. In northern Europe and Asia (including the majority of Russia), the IFI algorithm was solely used. However, further south down to 30°N, the IFI algorithm was used in unison with other algorithms, namely the UTL Europe algorithm for southern Europe and northern Africa, UTL Africa 2 in Turkey, Iraq and regions surrounding the Black and Caspian Seas and the UTL Asia (a derivative of UTL Africa 1) for a large region stretching between the Tibetan Plateau in the west through Mongolia and China to Japan in the east. The Indian sub-continent, southern China, continental and insular Southeast Asia were processed solely with the IFI algorithm. Australia was processed with an algorithm developed by GVM (developed by Stroppiana). Certain regions were not considered at all in the GBA, 2000 project because of their isolated location or their insignificant contribution to global burning activity. These regions include New Zealand and many small Pacific Islands, northern England, Scotland, Eire, Northern Ireland, Hawaii, Iceland and Greenland. The merits and performance of each of these algorithms is presented in Tansey (2002).

In certain regions, the algorithms were not applied to the VGT dataset for the whole of the year 2000. These regions were characterized by distinct fire seasons caused mainly by climatic variations (snow cover, heavy rainfall etc.). In more than one case, when the algorithms were applied to the VGT data outside the main periods of fire activity then false detections were observed, most commonly due to flooding. Information was used from published literature and other sources, for example the World Fire Web (Dwyer et al., 1999) to define the main periods of burning activity. To summarize, the main period of burning activity regions lying north of 30°N correspond to the Northern Hemisphere summer period, therefore data were processed between April and October 2000. South of this region and approximately between 30°N and 8°N in Central America, 30°N and 10°N in Africa and 30°N and 6°N in India and Southeast Asia the main period of burning activity is associated with the Northern Hemisphere dry season (winter), therefore data were processed between January and May 2000 and again from September to December 2000. In

the equatorial region and Southern Hemisphere the burning season is less distinct, apart from in Africa. In southern Africa, between approximately 10°S and the Cape of Good Hope in South Africa, the main period of burning is associated with the Southern Hemisphere dry season (winter), therefore data were processed between April and December 2000. The annual dataset was processed for all other regions including South America south of 10°N, equatorial Africa between 10°N and 10°S and insular Southeast Asia and Australia south of 6°N. In these regions there is potential for significant burning activity at any time of the year. The inventory described in the paper contains monthly burned area products and a synthesis of the total annual burned area for the year 2000 (the latter indicating those pixels detected as burned one or more times during the year 2000). During the processing of the data the monthly products were made non-accumulative. The assumption that, a vegetated surface burns only once during the year, is made in most regions. However, this is not always true, for example in Africa, in countries such as Chad, Sudan and Ethiopia, it may be that a vegetated area is burned towards the end of the 1999–2000 dry season so is detected in January 2000 and after the wet season and vigorous vegetation growth during this time, the vegetation is again burned earlier in the 2000–2001 dry season and is detected in December 2000. Therefore, a caution is given to the user when using the year 2000 synthesis product. This product may yield the total area burned during the year 2000, but if the user is using the product to infer burned biomass or emissions then errors are potentially introduced through an underestimation. The phenomenon of two detections during the year 2000 only affects those regions between 0 and 30°N. The ability to detect burnt areas that occur beneath a vegetated canopy that has not been burnt needs to be mentioned. It is believed that these burn scars are not detected by the VGT sensor because the main component of the radiant signal is coming from the part of the vegetation canopy that has not burnt. The chance of detecting the burn scar increases significantly as the density of the canopy decreases. Pereira et al. (in press) presents a discussion of this topic.

The masking of contaminated pixels before applying the algorithms was a necessary step for several of the algorithms. Contaminated pixels having values characteristic of clouds, cloud shadow (that have similar spectral characteristics to burned areas) and fire smoke are removed. In addition, those pixels located at the very edge of the image swath are removed because often they have erroneous values caused by the resampling method and also those that appear to be saturated (or have very high values of reflectance) in the short-wave infrared band caused by problems with the sensor. It was discovered that in regions of pronounced topographical variation, such as the Himalayas and the Andes, pixels were falsely being detected as being burnt in areas of terrain shadow. To solve this problem, a digital elevation model (a DEM from the Global Land One-km Base Elevation (GLOBE) product (Hastings and Dunbar, 1998) from <http://www.ndgc.noaa.gov/seg/topo/globe.shtml>), registered to the VGT S1 dataset was used. The method used to determine those pixels contaminated by terrain shadow is given by Colby (1991) and uses sun zenith and

azimuth information on a pixel basis provided in the VGT S1 product as well as slope and aspect information from the DEM. After determining the contaminated pixels, they were dilated by one-pixel in all directions to ensure that all shadow-affected pixels were removed. The terrain shadow masks were produced on a daily basis. Information on land cover at a global scale was used in this study for a number of reasons. A land cover product provides a mask to remove non-vegetated surfaces such as water, urban areas, deserts (including the Sahara, Kalahari, Arabian Peninsula, Tibetan Plateau and Atacama deserts) and ice masses that can otherwise cause problems and uncertainties in the performance of the algorithms. A land cover product provides guidance in the selection of an algorithm that is to be applied to a region of interest outside the region in which the algorithm was developed and calibrated. The global land cover product selected for this study was the University of Maryland (UMD) global land cover product (Hansen et al., 2000). The UMD product was selected because during the time that this study was undertaken it was considered to be the most current product that was freely available to the users (<http://glcf.umd.edu/data.html>) and actively being used by many different research groups.

4. Analysis and Discussion of the GBA, 2000 Inventory

The inventory described in this paper consists of one annual and twelve monthly products of burned areas at a resolution of 1 km. A detailed description is given of the spatial and temporal distribution of burned areas in the year 2000 overlapped with political boundaries. This method of reporting may primarily appeal to the policy decision-making community, but we believe that reporting the statistics in this way will best demonstrate the value of the GBA, 2000 dataset and encourage other users to use this data, particularly climate change and ecosystem modellers, for their own aims and objectives. Those interested in burnt area estimates for broad vegetation cover types (forest, grasslands and croplands, savannas and woodlands) should refer to Tansey et al. (2004). Following this description, discussion is presented on placing the year 2000 into context when considering burning activity in other years. The final sub-section describes some of the observed errors in the GBA, 2000 products and outlines validation exercises. All estimates of burned area are given in square kilometers (km²).

4.1. SPATIAL AND TEMPORAL DISTRIBUTION OF BURNED AREAS

The story of biomass burning in the year 2000 is shown in Figure 1. Figure 1 (top) shows the percentage of the total surface area (land and water) of each one-half degree (1/2°) cell burned in the year 2000. This parameter provides an indication of the magnitude (or inferred intensity) of biomass burning processes in each grid cell. The values range from one percent of the surface area to one hundred percent (at 1 km resolution) burning, the latter estimate occurring in several grid cells in

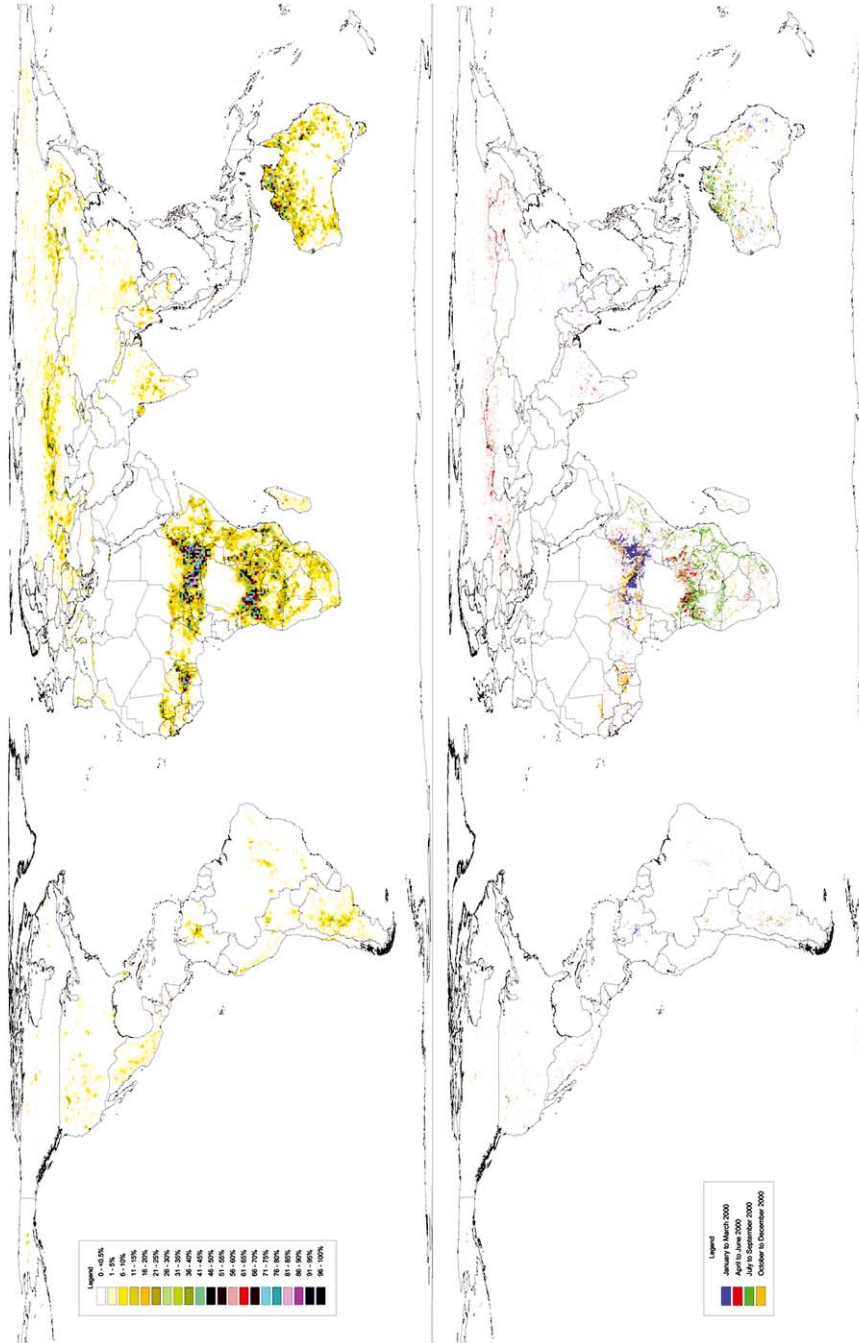


Figure 1. Global burned area maps of the year 2000. The image at the top indicates the percentage of the total surface area (both land and water areas) of each one-half degree cell burned in the year 2000. The image at the bottom shows the spatial and temporal distribution (three-month periods) of burned areas in the year 2000.

southern Sudan and the Central African Republic. As previously mentioned, the region with the greatest burning activity per surface area is the Northern Hemisphere sub-tropical shrubland and wooded grassland belt in Africa. With the exception of Somalia and Nigeria (for reasons that may be worthy of further investigation) biomass burning is widespread in this region. High intensities of burning activity is observed in the Southern Hemisphere of Africa, with peaks to be found in northern Angola and southern DR Congo (80% of the grid cell). Similar intensities can be found in northern Australia in the tropical grassland and interior regions. Moderate intensities of burning (30–60%) are observed in a number of places, including the temperate grasslands of eastern Mongolia and northern China and in southern China, Burma and isolated regions of India. The major grassland regions of South America (the Llanos of the Orinoco in Venezuela and Colombia, the Mato Grosso in Brazil, the Llanos of Mojos in Bolivia and the Pampas in Argentina) are all observed to have moderate intensities of burning activity. Burning activity in southwest Russia, the Ukraine and northern Kazakhstan also occurs in moderate intensities. This burning has been associated with agricultural practices. Other isolated hotspots are detected across the globe. Two regions highlighted are the large forest fires detected in Montana and Idaho States of the US in the year 2000 and the large forest fires in Canada that are large enough to represent a significant proportion of the one-half degree cell.

Figure 1 (bottom) shows the temporal distribution (in three month periods) of the burning activity in the year 2000 at global scale. Unlike the figure shown above it, Figure 1 (bottom) shows the actual pixels (resampled for display purposes) that were detected as being burned. Monthly maps of burned areas can be viewed through the Internet, hosted by the United Nation Environment Programme (UNEP) at <http://www.grid.unep.ch/activities/earlywarning/preview/ims/gba/>. In the following paragraphs, the use of the phrase 'burning activity' refers to the detection of burn scars and not the detection of active fires or fire activity.

Estimates of burned area (in square kilometers) are given in Table II by political boundary to support the statements that are made in the text. In addition to the burned area values, figures are presented on the number of burned scars (either single pixel or cluster of pixels) and the average size of a burned area (in square kilometers) and, for the year 2000, the percentage of the total area of the country (including land and water areas). The values given in Table II are comma delimited and are presented for each month of the year 2000 and for the year 2000 annual synthesis. A dash (-) indicates that no burned area product was derived for that particular month and country. Note that only those countries with burned scars detected in the year 2000 are presented in Table II. Countries that are absent from the table either have no burned areas detected within their political boundary or were not included when the algorithms were applied. Before an interpretation of the monthly distribution of burned areas is given it is worth extracting the main themes that are observed in the annual synthesis of the GBA, 2000 product. To help us to extract the main themes the GBA, 2000 products are cross-referenced with a

TABLE II
 Key (comma delimited): Burned area (km²), number of scars, average size of the scar (km²), % of total area of country burned (shown for the year 2000 only), a dash (-) indicates no data were acquired

	January	February	March	April	May	June	July	August	September	October	November	December	Year 2000
Afghanistan	-	-	-	19, 15, 1.2	17, 19, 0.9	124, 56, 2.2	184, 93, 2.0	281, 189, 1.5	5, 2, 2.4	56, 53, 1.1	-	-	686, 320, 2.1, 0.1
Albania	-	-	-	8, 6, 1.3	0, 0, 0	0, 0, 0	15, 5, 3.1	14, 6, 2.3	1, 2, 0.7	84, 50, 1.7	-	-	122, 67, 1.8, 0.4
Algeria	-	-	-	2, 1, 1.6	35, 15, 2.3	15, 15, 1.0	21, 17, 1.2	377, 80, 4.7	883, 174, 5.1	171, 92, 1.9	-	-	1503, 251, 6.0, 0.1
Angola	14, 1, 13.6	5, 3, 1.6	7, 3, 2.3	2670, 432, 6.2	4994, 887, 5.6	70341, 4399, 16.0	112482, 8415, 13.4	66005, 7950, 8.3	33158, 6194, 5.4	5165, 1380, 3.7	1212, 406, 3.0	511, 173, 3.0	296545, 20286, 14.6, 23.7
Argentina	3168, 1195, 2.7	3049, 1558, 2.0	2468, 1032, 2.4	3972, 1921, 2.1	8807, 3565, 2.5	4157, 2140, 1.9	7653, 3382, 2.3	5173, 2905, 1.8	5559, 2372, 2.3	1574, 688, 2.3	3194, 1120, 2.9	6696, 886, 7.6	55468, 16717, 3.3, 2.0
Armenia	-	-	-	61, 28, 2.2	0, 0, 0	2, 1, 2.3	6, 5, 1.2	9, 6, 1.5	0, 0, 0	0, 0, 0	-	-	79, 38, 2.1, 0.3
Australia	45263, 2777, 16.3	27515, 2086, 13.2	16924, 1672, 10.1	10740, 1207, 8.9	13995, 1169, 12.0	22581, 1569, 14.4	28167, 1480, 19.0	69616, 1666, 41.8	140393, 2314, 60.7	84243, 2601, 32.4	85698, 3984, 21.5	13732, 957, 14.3	558867, 19693, 284, 7.3
Austria	-	-	-	4, 1, 4.0	0, 0, 0	0, 0, 0	5, 4, 1.2	1, 1, 0.7	34, 37, 0.9	53, 26, 2.0	-	-	96, 68, 1.4, 0.1
Azerbaijan	-	-	-	189, 63, 3.0	18, 14, 1.3	31, 14, 2.2	143, 51, 2.8	146, 49, 3.0	0, 0, 0	4, 3, 1.3	-	-	531, 174, 3.1, 0.6
Bahamas	0, 0, 0	0, 0, 0	0, 0, 0	7, 2, 3.5	1, 1, 0.9	-	-	-	0, 0, 0	0, 0, 0	1, 1, 0.9	0, 0, 0	9, 4, 2.2, 0.1
Bangladesh	66, 12, 5.5	17, 13, 1.3	24, 5, 4.7	43, 5, 8.7	11, 2, 5.4	-	-	-	0, 0, 0	3, 2, 1.3	59, 7, 8.5	54, 9, 6.0	277, 49, 5.7, 0.2
Belgium	-	-	-	10, 1, 9.6	0, 0, 0	0, 0, 0	0, 0, 0	0, 0, 0	0, 0, 0	0, 0, 0	-	-	10, 1, 9.6, 0
Belize	0, 0, 0	0, 0, 0	0, 0, 0	0, 0, 0	0, 0, 0	-	-	-	0, 0, 0	0, 0, 0	0, 0, 0	1, 1, 0.9	1, 1, 0.9, 0
Benin	1581, 347, 4.6	282, 113, 2.5	4, 3, 1.3	54, 32, 1.7	15, 7, 2.1	1, 1, 1.0	0, 0, 0	0, 0, 0	3, 3, 1.0	0, 0, 0	1769, 189, 9.4	9943, 805, 12.4	13003, 1194, 10.9, 11.2
Bhutan	3, 3, 1.2	3, 2, 1.7	15, 4, 3.7	52, 8, 6.4	0, 0, 0	-	-	-	0, 0, 0	26, 7, 3.7	24, 10, 2.4	33, 14, 2.4	156, 46, 3.4, 0.4
Bolivia	36, 23, 1.6	49, 35, 1.4	22, 22, 1.0	186, 146, 1.3	786, 447, 1.8	360, 248, 1.5	2196, 608, 3.6	1651, 514, 3.2	3516, 477, 7.4	685, 149, 4.6	383, 195, 2.0	315, 177, 1.8	10185, 2539, 4.0, 0.9

(Continued on next page)

TABLE II
(Continued)

	January	February	March	April	May	June	July	August	September	October	November	December	Year 2000
Botswana	-	-	-	647, 267, 2.4	1418, 727, 2.0	10106, 3833, 2.6	556, 235, 2.4	1697, 287, 5.9	6003, 832, 7.2	11865, 901, 13.2	1010, 199, 5.1	248, 79, 3.1	33550, 6472, 5.2, 5.8
Brazil	92, 67, 1.4	38, 31, 1.2	566, 439, 1.3	197, 155, 1.3	359, 183, 2.0	1721, 501, 3.4	2910, 803, 3.6	7400, 1529, 4.8	2500, 565, 4.4	2294, 316, 7.3	103, 87, 1.2	114, 81, 1.4	18293, 4414, 4.1, 0.2
Bulgaria	-	-	-	117, 73, 1.6	2, 3, 0.7	71, 56, 1.3	119, 29, 4.1	763, 253, 3.0	340, 214, 1.6	709, 290, 2.4	-	-	2121, 685, 3.1, 1.9
Burkina Faso	1718, 591, 2.9	267, 156, 1.7	52, 31, 1.7	113, 68, 1.7	103, 64, 1.6	0, 0, 0	0, 0, 0	0, 0, 0	0, 0, 0	549, 270, 2.0	6999, 1082, 6.5	6856, 982, 7.0	15813, 2549, 6.2, 5.8
Burundi	0, 0, 0	2, 2, 1.0	0, 0, 0	0, 0, 0	2, 1, 2.0	160, 29, 5.5	314, 74, 4.2	147, 48, 3.1	72, 22, 3.3	25, 13, 1.9	0, 0, 0	0, 0, 0	721, 168, 4.3, 2.6
Byelarus	-	-	-	370, 326, 1.1	11, 16, 0.7	11, 9, 1.3	0, 0, 0	0, 0, 0	1, 2, 0.6	78, 73, 1.1	-	-	472, 394, 1.2, 0.2
Cambodia	755, 97, 7.8	3006, 251, 12.0	79, 18, 4.4	9, 3, 2.9	9, 4, 2.2	-	-	-	0, 0, 0	0, 0, 0	0, 0, 0	21, 5, 4.2	3867, 307, 12.6, 2.1
Cameroon	8242, 1049, 7.9	2071, 478, 4.3	1756, 417, 4.2	752, 316, 2.4	860, 386, 2.2	1, 1, 1.0	3, 3, 1.0	15, 11, 1.3	86, 41, 2.1	496, 115, 4.3	6676, 915, 7.3	33315, 1757, 19.0	49928, 3458, 14.4, 10.7
Canada	-	-	-	20, 22, 0.9	23, 30, 0.8	254, 210, 1.2	1355, 417, 3.2	2824, 548, 5.2	1207, 901, 1.3	4, 5, 0.8	-	-	5687, 625, 9.1, 0.1
Cent. African Rep.	95668, 5088, 18.8	8635, 1149, 7.5	1224, 219, 5.6	177, 34, 5.2	31, 8, 3.9	0, 0, 0	4, 4, 1.0	0, 0, 0	9, 3, 2.9	78, 17, 4.6	11216, 874, 12.8	99095, 4679, 21.2	185479, 7592, 24.4, 30.0
Chad	13457, 1995, 6.7	6053, 1819, 3.3	2712, 884, 3.1	1049, 474, 2.2	1999, 875, 2.3	0, 0, 0	0, 0, 0	10, 3, 3.2	3, 2, 1.5	19484, 2916, 6.7	18046, 2816, 6.4	23950, 2503, 9.6	80728, 10235, 7.9, 6.3
Chile	349, 187, 1.9	375, 302, 1.2	457, 276, 1.7	368, 264, 1.4	421, 279, 1.5	131, 109, 1.2	98, 90, 1.1	24, 20, 1.2	17, 16, 1.0	3, 4, 0.9	107, 83, 1.3	185, 127, 1.5	2536, 1282, 2.0, 0.3
China	3084, 673, 4.6	4335, 858, 5.1	6324, 788, 8.0	19084, 3661, 5.2	9631, 2606, 3.7	6449, 2039, 3.2	1867, 720, 2.6	1466, 844, 1.7	1089, 532, 2.0	6348, 2000, 3.2	1561, 404, 3.9	1619, 478, 3.4	62388, 13049, 4.8, 0.7
Colombia	2068, 342, 6.0	4523, 288, 15.7	2904, 205, 14.2	0, 0, 0	1, 1, 1.0	9, 9, 1.0	18, 14, 1.3	2, 2, 1.0	0, 0, 0	7, 4, 1.7	10, 7, 1.4	98, 50, 2.0	9627, 814, 11.8, 0.8

Comoros	-	-	-	11, 6, 1.8	10, 5, 1.9	2, 2, 1.0	1, 1, 1.0	11, 4, 2.6	1, 1, 1.0	1, 1, 1.0	-	-	36, 13, 2.7, 2.2
Congo	28, 15, 1.9	29, 18, 1.6	79, 40, 2.0	89, 29, 3.1	40, 13, 3.1	266, 40, 6.6	1221, 245, 5.0	1211, 296, 4.1	1492, 195, 7.7	1021, 66, 15.5	381, 85, 4.5	5, 5, 1.0	5810, 797, 7.3, 1.7
Costa Rica	0, 0, 0	3, 2, 1.4	0, 0, 0	44, 13, 3.4	0, 0, 0	-	-	-	0, 0, 0	0, 0, 0	4, 3, 1.3	0, 0, 0	51, 18, 2.8, 0.1
Cuba	50, 18, 2.8	130, 47, 2.8	82, 26, 3.1	190, 65, 2.9	55, 17, 3.3	-	-	-	0, 0, 0	0, 0, 0	7, 3, 2.4	3, 3, 0.9	513, 144, 3.6, 0.5
Cyprus	-	-	-	0, 0, 0	4, 3, 1.3	20, 5, 4.0	0, 0, 0	2, 2, 0.8	0, 0, 0	0, 0, 0	-	-	26, 10, 2.6, 0.3
Czech Rep-Slovak.	-	-	-	34, 14, 2.5	0, 0, 0	1, 2, 0.7	0, 0, 0	0, 0, 0	20, 15, 1.3	143, 51, 2.8	-	-	199, 78, 2.6, 0.2
Dem. Rep. Congo	15288, 1404, 10.9	6763, 1094, 6.2	1866, 360, 5.2	295, 145, 2.0	26225, 2980, 8.8	90478, 6952, 13.0	87739, 7178, 12.2	24265, 2590, 9.4	3653, 796, 4.6	476, 176, 2.7	490, 179, 2.7	4588, 469, 9.8	260032, 15614, 16.7, 11.2
Djibouti	7, 6, 1.1	94, 20, 4.7	0, 0, 0	6, 4, 1.4	5, 2, 2.4	-	-	-	0, 0, 0	317, 37, 8.6	27, 13, 2.1	0, 0, 0	421, 45, 9.4, 2.0
Dominican Rep.	1, 1, 0.9	4, 3, 1.2	7, 5, 1.3	0, 0, 0	0, 0, 0	-	-	-	0, 0, 0	0, 0, 0	3, 2, 1.4	2, 2, 0.9	16, 12, 1.3, 0
Ecuador	6, 6, 1.0	25, 20, 1.2	13, 13, 1.0	3, 2, 1.5	4, 4, 1.0	28, 25, 1.1	42, 29, 1.5	30, 22, 1.4	13, 9, 1.4	11, 5, 2.2	7, 7, 1.0	16, 11, 1.4	197, 138, 1.4, 0.1
Egypt	-	-	-	18, 7, 2.5	812, 83, 9.8	78, 45, 1.7	4, 4, 1.1	0, 0, 0	0, 0, 0	0, 0, 0	-	-	912, 125, 7.3, 0.1
El Salvador	9, 5, 1.7	5, 4, 1.2	0, 0, 0	0, 0, 0	0, 0, 0	-	-	-	0, 0, 0	0, 0, 0	3, 1, 2.9	3, 3, 1.0	16, 6, 2.7, 0.1
Equatorial Guinea	11, 2, 5.4	0, 0, 0	0, 0, 0	7, 5, 1.4	0, 0, 0	0, 0, 0	0, 0, 0	0, 0, 0	0, 0, 0	2, 1, 2.0	0, 0, 0	0, 0, 0	19, 6, 3.1, 0.1
Estonia	-	-	-	7, 11, 0.7	17, 14, 1.2	1, 1, 0.5	0, 0, 0	0, 0, 0	1, 1, 0.5	0, 0, 0	-	-	25, 26, 1.0, 0.1
Ethiopia	29344, 2482, 11.8	19906, 2419, 8.2	22160, 2540, 8.7	11470, 2621, 4.4	6288, 1565, 4.0	2684, 748, 3.6	3234, 1246, 2.6	10504, 2412, 4.4	4374, 1588, 2.8	4124, 1244, 3.3	8764, 1428, 6.1	29341, 4429, 6.6	140919, 15660, 9.0, 11.3
Finland	-	-	-	7, 11, 0.7	78, 124, 0.6	10, 17, 0.6	4, 6, 0.7	0, 1, 0.3	0, 0, 0	0, 0, 0	-	-	99, 158, 0.6, 0
France	-	-	-	80, 35, 2.3	1, 1, 0.7	13, 14, 0.9	59, 45, 1.3	48, 35, 1.4	238, 115, 2.1	117, 84, 1.4	-	-	555, 282, 2.0, 0.1
French Guiana	0, 0, 0	0, 0, 0	0, 0, 0	0, 0, 0	0, 0, 0	1, 1, 1.0	0, 0, 0	0, 0, 0	0, 0, 0	0, 0, 0	0, 0, 0	0, 0, 0	1, 1, 1.0, 0
Gabon	22, 12, 1.8	21, 6, 3.4	12, 8, 1.5	47, 14, 3.4	58, 10, 5.8	4, 2, 2.0	105, 32, 3.3	534, 136, 3.9	4, 1, 3.9	0, 0, 0	0, 0, 0	0, 0, 0	805, 199, 4.0, 0.3

(Continued on next page)

TABLE II
(Continued)

	January	February	March	April	May	June	July	August	September	October	November	December	Year 2000
Gambia	79, 18, 4.4	477, 40, 11.9	63, 17, 3.7	24, 14, 1.7	114, 63, 1.8	-	-	-	0, 0, 0	4, 3, 1.3	72, 21, 3.4	21, 12, 1.7	814, 148, 5.5, 7.6
Georgia	-	-	-	59, 17, 3.4	12, 7, 1.8	15, 8, 1.9	28, 12, 2.3	61, 45, 1.4	0, 0, 0	5, 3, 1.7	-	-	181, 85, 2.1, 0.3
Germany	-	-	-	25, 16, 1.6	3, 3, 1.0	0, 0, 0	0, 0, 0	7, 2, 3.4	22, 10, 2.2	13, 12, 1.1	-	-	70, 39, 1.8, 0
Ghana	9775, 1933, 5.1	1024, 369, 2.8	167, 87, 1.9	23, 17, 1.4	43, 23, 1.9	0, 0, 0	3, 2, 1.5	0, 0, 0	0, 0, 0	12, 11, 1.1	4398, 531, 8.3	42073, 1372, 30.7	53747, 2374, 22.6, 22.5
Greece	-	-	-	12, 5, 2.4	2, 2, 1.2	29, 29, 1.0	469, 46, 10.2	186, 31, 6.0	71, 37, 1.9	396, 118, 3.4	-	-	1165, 231, 5.0, 0.9
Guatemala	36, 28, 1.3	54, 39, 1.4	5, 3, 1.6	45, 12, 3.8	0, 0, 0	-	-	-	0, 0, 0	0, 0, 0	0, 0, 0	13, 7, 1.9	152, 82, 1.9, 0.1
Guinea	2174, 613, 3.5	1532, 452, 3.4	146, 64, 2.3	53, 23, 2.3	9, 7, 1.2	0, 0, 0	0, 0, 0	0, 0, 0	0, 0, 0	46, 14, 3.3	287, 91, 3.2	3923, 757, 5.2	7999, 1807, 4.4, 3.3
Guinea-Bissau	100, 33, 3.0	197, 66, 3.0	4, 3, 1.3	14, 6, 2.4	39, 23, 1.7	-	-	-	0, 0, 0	0, 0, 0	37, 22, 1.7	13, 9, 1.5	393, 145, 2.7, 1.2
Guyana	0, 0, 0	1, 1, 1.0	0, 0, 0	0, 0, 0	0, 0, 0	1, 1, 1.0	1, 1, 1.0	0, 0, 0	0, 0, 0	0, 0, 0	0, 0, 0	0, 0, 0	3, 3, 1.0, 0
Haiti	7, 3, 2.5	14, 5, 2.8	1, 1, 0.9	0, 0, 0	0, 0, 0	-	-	-	0, 0, 0	0, 0, 0	0, 0, 0	2, 1, 1.9	22, 8, 2.8, 0.1
Honduras	2, 2, 1.0	13, 2, 6.7	0, 0, 0	2, 2, 1.0	0, 0, 0	-	-	-	0, 0, 0	0, 0, 0	0, 0, 0	1, 1, 1.0	18, 7, 2.6, 0
Hungary	-	-	-	52, 50, 1.0	16, 15, 1.1	14, 18, 0.8	4, 4, 1.0	99, 55, 1.8	640, 310, 2.1	554, 271, 2.0	-	-	1378, 550, 2.5, 1.5
India	3917, 455, 8.6	3066, 496, 6.2	12937, 1075, 12.0	9549, 1011, 9.4	8917, 878, 10.2	0, 0, 0	0, 0, 0	37, 6, 6.1	555, 75, 7.4	3179, 606, 5.2	2922, 356, 8.2	5399, 670, 8.1	47134, 3268, 14.4, 1.5
Indonesia	12, 2, 5.9	10, 2, 4.9	6, 3, 2.0	57, 3, 18.9	15, 2, 7.3	66, 6, 11.1	77, 16, 4.8	513, 75, 6.8	916, 107, 8.6	204, 23, 8.9	16, 3, 5.2	11, 3, 3.6	1902, 188, 10.1, 0.1
Iran	-	-	-	620, 235, 2.6	30, 21, 1.5	99, 60, 1.6	100, 57, 1.7	185, 103, 1.8	0, 0, 0	8, 2, 3.9	-	-	1042, 418, 2.5, 0.1
Iraq	-	-	-	17, 11, 1.5	6, 6, 0.9	0, 0, 0	0, 0, 0	22, 11, 2.0	0, 0, 0	0, 0, 0	-	-	44, 28, 1.6, 0

Italy	-	-	-	144, 53, 2.7	2, 2, 0.8	1289, 468, 2.8	108, 45, 2.4	191, 102, 1.9	565, 258, 2.2	218, 120, 1.8	-	-	2516, 875, 2.9, 0.8
Ivory Coast	2768, 523, 5.3	-	534, 147, 3.6	26, 13, 2.0	24, 15, 1.6	0, 0, 0	0, 0, 0	0, 0, 0	0, 0, 0	0, 0, 0	86, 28, 3.1	18615, 930, 20.0	20990, 1339, 15.7, 6.5
Japan	-	-	-	173, 26, 6.6	860, 274, 3.1	2, 1, 1.7	86, 35, 2.5	67, 41, 1.6	0, 0, 0	0, 0, 0	-	-	1188, 375, 3.2, 0.3
Kazakhstan	-	-	-	37811, 9007, 4.2	6668, 3120, 2.1	6192, 2613, 2.4	4248, 1603, 2.6	16836, 3193, 5.3	8546, 1789, 4.8	1322, 811, 1.6	-	-	81622, 17571, 4.6, 3.0
Kenya	9745, 1471, 6.6	-	746, 300, 2.5	3226, 574, 5.6	7283, 1549, 4.7	2180, 846, 2.6	4087, 1021, 4.0	6701, 2001, 3.3	13903, 2997, 4.6	4569, 1501, 3.0	1105, 338, 3.3	5021, 1062, 4.7	57654, 8364, 6.9, 9.9
Korea (North)	-	-	-	1057, 161, 6.6	901, 140, 6.4	0, 0, 0	2, 2, 0.8	0, 0, 0	0, 0, 0	693, 119, 5.8	-	-	2653, 384, 6.9, 2.2
Korea (South)	-	-	-	453, 33, 13.7	0, 0, 0	0, 0, 0	1, 1, 0.8	56, 17, 3.3	0, 0, 0	0, 0, 0	-	-	510, 51, 10.0, 0.5
Kyrgyzstan	-	-	-	20, 8, 2.5	6, 5, 1.2	17, 14, 1.2	90, 56, 1.6	828, 381, 2.2	63, 53, 1.2	44, 20, 2.2	-	-	1067, 469, 2.3, 0.5
Laos	473, 69, 6.9	-	480, 91, 5.3	18, 4, 4.4	0, 0, 0	-	-	0, 0, 0	0, 0, 0	25, 4, 6.3	411, 20, 20.6	269, 76, 3.5	1474, 124, 11.9, 0.6
Latvia	-	-	-	50, 29, 1.7	4, 4, 0.9	0, 0, 0	0, 0, 0	0, 0, 0	0, 0, 0	0, 0, 0	-	-	54, 33, 1.6, 0.1
Lesotho	-	-	-	337, 163, 2.1	226, 159, 1.4	242, 149, 1.6	165, 112, 1.5	517, 117, 4.4	206, 78, 2.6	12, 10, 1.2	0, 0, 0	19, 9, 2.1	1723, 678, 2.5, 5.7
Liberia	0, 0, 0	-	0, 0, 0	1, 1, 1.0	0, 0, 0	0, 0, 0	0, 0, 0	0, 0, 0	0, 0, 0	0, 0, 0	0, 0, 0	0, 0, 0	2, 2, 1.0, 0
Liechtenstein	-	-	-	0, 0, 0	0, 0, 0	0, 0, 0	0, 0, 0	0, 0, 0	0, 0, 0	3, 2, 1.7	-	-	3, 2, 1.7, 2.0
Lithuania	-	-	-	12, 9, 1.4	0, 0, 0	0, 0, 0	0, 0, 0	0, 0, 0	0, 0, 0	0, 0, 0	-	-	12, 9, 1.4, 0
Madagascar	-	-	-	82, 38, 2.2	433, 230, 1.9	1592, 464, 3.4	1178, 414, 2.8	1775, 618, 2.9	2916, 1121, 2.6	1899, 673, 2.8	1062, 508, 2.1	399, 165, 2.4	11336, 3804, 3.0, 1.9
Malawi	-	-	-	11, 8, 1.3	83, 20, 4.1	78, 30, 2.6	1614, 232, 7.0	699, 189, 3.7	2040, 645, 3.2	733, 404, 1.8	157, 92, 1.7	71, 18, 4.0	5487, 1347, 4.1, 4.6

(Continued on next page)

TABLE II
(Continued)

	January	February	March	April	May	June	July	August	September	October	November	December	Year 2000
Malaysia	0, 0, 0	0, 0, 0	6, 1, 5.9	0, 0, 0	0, 0, 0	0, 0, 0	25, 2, 12.7	0, 0, 0	0, 0, 0	0, 0, 0	0, 0, 0	0, 0, 0	31, 3, 10.4, 0
Mali	4034, 1832, 2.2	1064, 623, 1.7	882, 372, 2.4	471, 210, 2.2	586, 307, 1.9	-	-	-	0, 0, 0	3747, 812, 4.6	8608, 2305, 3.7	3134, 879, 3.6	21809, 5669, 3.8, 1.7
Mauritania	367, 252, 1.5	21, 15, 1.4	249, 27, 9.2	372, 12, 31.0	24, 14, 1.7	-	-	-	0, 0, 0	8515, 912, 9.3	6800, 1372, 5.0	901, 199, 4.5	16811, 1720, 9.8, 1.6
Mexico	2967, 1649, 1.8	3193, 1595, 2.0	1864, 691, 2.7	1861, 408, 4.6	2377, 548, 4.3	2, 2, 0.8	15, 7, 2.2	7, 6, 1.1	9, 6, 1.5	1876, 748, 2.5	4082, 1715, 2.4	3964, 1969, 2.0	21226, 6765, 3.1, 1.1
Moldova	-	-	-	206, 162, 1.3	23, 22, 1.1	2, 3, 0.7	5, 7, 0.7	134, 83, 1.6	200, 120, 1.7	506, 305, 1.7	-	-	1076, 534, 2.0, 3.2
Mongolia	-	-	-	7597, 674, 11.3	13688, 1121, 12.2	2844, 805, 3.5	1039, 591, 1.8	1186, 706, 1.7	86, 79, 1.1	117, 76, 1.5	-	-	26556, 2933, 9.1, 1.7
Monocco	-	-	-	287, 122, 2.3	372, 123, 3.0	107, 48, 2.2	375, 129, 2.9	39, 29, 1.4	341, 209, 1.6	727, 343, 2.1	-	-	2247, 500, 4.5, 0.6
Mozambique	-	-	-	772, 179, 4.3	190, 87, 2.2	655, 196, 3.3	15818, 1675, 9.4	32812, 3457, 9.5	32074, 5034, 6.4	19765, 3197, 6.2	464, 162, 2.9	69, 38, 1.8	102618, 10971, 9.4, 13.1
Myanmar	2191, 154, 14.2	877, 145, 6.0	3608, 290, 12.4	4241, 421, 10.1	43, 8, 5.4	-	-	-	0, 0, 0	5, 1, 5.4	68, 10, 6.8	88, 26, 3.4	11086, 764, 14.5, 1.7
Namibia	-	-	-	2408, 377, 6.4	4771, 2676, 1.8	1788, 1206, 1.5	1928, 1017, 1.9	3997, 867, 4.6	12745, 2604, 4.9	3627, 904, 4.0	2082, 318, 6.5	1750, 869, 2.0	35097, 9338, 3.8, 4.3
Nepal	66, 31, 2.1	85, 50, 1.7	858, 241, 3.6	718, 118, 6.1	58, 17, 3.4	0, 0, 0	0, 0, 0	0, 0, 0	14, 4, 3.4	957, 157, 6.1	152, 66, 2.3	155, 56, 2.8	2987, 569, 5.3, 2.0
Nicaragua	32, 18, 1.8	16, 12, 1.4	0, 0, 0	10, 3, 3.2	0, 0, 0	-	-	-	0, 0, 0	0, 0, 0	1, 1, 1.0	5, 5, 1.0	62, 32, 1.9, 0
Niger	114, 54, 2.1	56, 16, 3.5	18, 2, 9.0	13, 10, 1.3	12, 4, 3.1	-	-	-	0, 0, 0	1150, 332, 3.5	1898, 698, 2.7	184, 106, 1.7	3409, 947, 3.6, 0.3
Nigeria	7499, 2581, 2.9	5144, 1745, 2.9	567, 248, 2.3	867, 449, 1.9	1413, 593, 2.4	9, 6, 1.5	11, 6, 1.8	8, 5, 1.6	3, 3, 1.0	3235, 554, 5.8	3027, 976, 3.1	11399, 2012, 5.7	31968, 7529, 4.2, 3.5

Norway	-	-	2, 3, 0.5	145, 123, 1.2	9, 15, 0.6	3, 6, 0.5	3, 4, 0.7	0, 0, 0	0, 0, 0	-	-	161, 150, 1.1, 0.1
Pakistan	24, 5, 4.9	13, 3, 4.4	4, 2, 2.1	12, 4, 3.0	13, 13, 1.0	11, 8, 1.4	43, 29, 1.5	11, 13, 0.9	276, 144, 1.9	29, 10, 2.9	11, 3, 3.8	449, 228, 2.0, 0.1
Papua New Guinea	0, 0, 0	0, 0, 0	0, 0, 0	0, 0, 0	0, 0, 0	0, 0, 0	26, 9, 2.9	96, 17, 5.7	0, 0, 0	5, 2, 2.4	0, 0, 0	132, 29, 4.6, 0
Paraguay	718, 116, 6.2	75, 48, 1.6	80, 33, 2.4	55, 19, 2.9	32, 22, 1.5	0, 0, 0	270, 111, 2.4	49, 23, 2.1	18, 14, 1.3	1, 1, 0.9	2, 1, 1.8	1326, 351, 3.8, 0.3
Peru	276, 61, 4.5	200, 161, 1.2	189, 141, 1.3	388, 234, 1.5	1944, 1006, 1.9	359, 231, 1.6	474, 217, 2.2	117, 84, 1.4	38, 32, 1.2	533, 306, 1.7	48, 32, 1.5	6547, 2934, 2.2, 0.5
Philippines	4, 1, 3.8	0, 0, 0	0, 0, 0	0, 0, 0	0, 0, 0	0, 0, 0	0, 0, 0	0, 0, 0	0, 0, 0	0, 0, 0	0, 0, 0	4, 1, 3.8, 0
Poland	-	-	-	77, 66, 1.2	2, 1, 2.5	1, 1, 1.3	1, 1, 0.6	2, 2, 1.0	82, 27, 3.0	-	-	165, 98, 1.7, 0.1
Portugal	-	-	-	6, 5, 1.2	8, 6, 1.4	91, 61, 1.5	369, 86, 4.3	211, 111, 1.9	154, 65, 2.4	-	-	885, 292, 3.0, 1.0
Romania	-	-	-	441, 224, 2.0	20, 19, 1.0	84, 76, 1.1	202, 126, 1.6	770, 267, 2.9	2027, 524, 3.9	-	-	3615, 1106, 3.3, 1.5
Russia	-	-	-	99927, 22720, 4.4	75820, 24714, 3.1	16005, 11396, 1.4	7897, 3359, 1.6	3186, 2561, 1.2	6309, 3538, 1.8	-	-	223575, 66213, 3.4, 1.3
Rwanda	0, 0, 0	25, 10, 2.5	12, 4, 2.9	0, 0, 0	4, 2, 2.0	154, 12, 12.8	113, 34, 3.3	37, 20, 1.9	26, 18, 1.5	0, 0, 0	0, 0, 0	603, 107, 5.6, 2.4
Senegal	2455, 375, 6.5	2882, 580, 5.0	365, 98, 3.7	149, 66, 2.3	516, 267, 1.9	-	-	0, 0, 0	109, 55, 2.0	3324, 715, 4.6	1957, 483, 4.1	11377, 2226, 5.1, 5.8
Seychelles	-	-	-	0, 0, 0	2, 1, 1.9	0, 0, 0	0, 0, 0	0, 0, 0	6, 2, 2.9	0, 0, 0	0, 0, 0	9, 1, 8.7, 3.4
Sierra Leone	14, 11, 1.2	983, 148, 6.6	11, 5, 2.1	2, 2, 1.0	2, 1, 1.9	2, 2, 1.0	0, 0, 0	0, 0, 0	2, 2, 1.0	0, 0, 0	13, 8, 1.6	1026, 177, 5.8, 1.4
Somalia	2614, 997, 2.6	229, 170, 1.3	238, 171, 1.4	184, 124, 1.5	38, 30, 1.3	95, 42, 2.3	1544, 512, 3.0	6024, 1262, 4.8	703, 320, 2.2	463, 181, 2.6	6753, 1249, 5.4	18319, 4211, 4.4, 2.9
South Africa	-	-	-	887, 635, 1.4	2542, 1844, 1.4	17120, 8238, 2.1	10109, 2570, 3.9	19752, 4134, 4.8	4459, 1578, 2.8	7824, 4141, 1.9	1517, 1080, 1.4	73727, 22780, 3.2, 6.0

(Continued on next page)

TABLE II
(Continued)

	January	February	March	April	May	June	July	August	September	October	November	December	Year 2000
Spain	-	-	-	60, 42, 1.4	37, 24, 1.5	331, 239, 1.4	151, 135, 1.1	321, 97, 3.3	564, 183, 3.1	215, 149, 1.4	-	-	1678, 707, 2.4, 0.3
Sri Lanka	0, 0, 0	0, 0, 0	0, 0, 0	0, 0, 0	20, 4, 5.1	-	-	-	3, 1, 2.9	15, 4, 3.7	0, 0, 0	3, 1, 2.9	38, 9, 4.2, 0.1
Sudan	140950, 5919, 23.8	42871, 3855, 11.1	23072, 3101, 7.4	10012, 3099, 3.2	11276, 3291, 3.4	1218, 283, 4.3	172, 74, 2.3	1944, 408, 4.8	649, 114, 5.7	12433, 1848, 6.7	63246, 5355, 11.8	169389, 6232, 27.2	403099, 17813, 22.6, 16.2
Swaziland	-	-	-	1, 1, 0.9	2, 2, 0.9	11, 4, 2.9	218, 49, 4.4	68, 25, 2.7	179, 51, 3.5	4, 2, 2.2	0, 0, 0	0, 0, 0	483, 125, 3.9, 2.8
Sweden	-	-	-	23, 31, 0.7	59, 69, 0.9	22, 27, 0.8	0, 1, 0.5	0, 0, 0	0, 0, 0	0, 0, 0	-	-	103, 127, 0.8, 0
Switzerland	-	-	-	1, 1, 0.7	0, 0, 0	0, 0, 0	0, 0, 0	1, 2, 0.7	13, 15, 0.9	3, 3, 0.9	-	-	18, 21, 0.8, 0
Syria	-	-	-	18, 11, 1.7	1, 1, 0.8	6, 4, 1.4	8, 8, 1.0	6, 4, 1.5	0, 0, 0	0, 0, 0	-	-	39, 27, 1.4, 0
Tajikistan	-	-	-	2, 2, 0.8	0, 0, 0	42, 13, 3.2	102, 54, 1.9	285, 164, 1.7	2, 3, 0.8	16, 15, 1.1	-	-	449, 203, 2.2, 0.3
Tanzania	1595, 451, 3.5	1118, 349, 3.2	686, 256, 2.7	465, 188, 2.5	5969, 896, 6.7	35267, 2687, 13.1	29900, 4539, 6.6	17673, 3801, 4.6	12465, 4241, 2.9	13122, 3302, 4.0	5627, 1733, 3.2	295, 123, 2.4	121969, 14529, 8.4, 13.0
Thailand	468, 121, 3.9	964, 159, 6.1	118, 33, 3.6	230, 30, 7.7	22, 2, 10.9	-	-	-	0, 0, 0	25, 4, 6.4	33, 10, 3.3	122, 51, 2.4	1971, 329, 6.0, 0.4
Togo	975, 304, 3.2	70, 60, 1.2	33, 19, 1.7	28, 15, 1.9	0, 0, 0	4, 1, 3.9	0, 0, 0	0, 0, 0	0, 0, 0	40, 21, 1.9	134, 68, 2.0	5407, 702, 7.7	6420, 933, 6.9, 11.2
Tunisia	-	-	-	1, 1, 0.8	14, 10, 1.4	1, 1, 0.8	1, 1, 0.8	10, 3, 3.4	50, 10, 5.0	13, 8, 1.6	-	-	89, 29, 3.1, 0.1
Turkey	-	-	-	136, 69, 2.0	486, 277, 1.8	782, 219, 3.6	220, 125, 1.8	273, 156, 1.7	51, 14, 3.7	820, 147, 5.6	-	-	2768, 815, 3.4, 0.4
Turkmenistan	-	-	-	14, 5, 2.8	120, 10, 12.0	25, 9, 2.7	57, 8, 7.1	18, 14, 1.3	0, 0, 0	0, 0, 0	-	-	233, 36, 6.5, 0
Uganda	19946, 1123, 17.8	3643, 502, 7.3	752, 300, 2.5	540, 264, 2.0	216, 99, 2.2	56, 17, 3.3	304, 50, 6.1	182, 74, 2.5	96, 46, 2.1	27, 14, 2.0	187, 60, 3.1	8660, 629, 13.8	31392, 2049, 15.3, 13.0
Ukraine	-	-	-	14980, 3832, 3.9	1553, 1292, 1.2	230, 203, 1.1	400, 282, 1.4	2575, 1192, 2.2	486, 330, 1.5	1713, 1041, 1.6	-	-	21938, 6890, 3.2, 3.7

United Kingdom	-	-	-	2, 1, 2.5	0, 0, 0	0, 0, 0	0, 0, 0	1, 1, 0.6	0, 0, 0	3, 3, 1.0	-	-	6, 5, 1.2, 0
Uruguay	17, 18, 0.9	12, 10, 1.2	1, 1, 0.8	11, 5, 2.2	5, 4, 1.2	0, 0, 0	11, 10, 1.1	16, 15, 1.1	5, 4, 1.3	1, 1, 0.8	1, 1, 0.8	4, 5, 0.8	83, 64, 1.3,
USA (incl. Alaska)	688, 295, 2.3	1538, 558, 2.8	141, 83, 1.7	3512, 1553, 2.3	1839, 969, 1.9	1607, 990, 1.6	4917, 1496, 3.3	5066, 1702, 3.0	14789, 4453, 3.3	227, 224, 1.0	312, 180, 1.7	518, 196, 2.6	34963, 9566, 3.7, 0.4
Uzbekistan	-	-	-	67, 60, 1.1	68, 63, 1.1	7, 8, 0.9	53, 36, 1.5	272, 114, 2.4	5, 7, 0.8	33, 26, 1.3	-	-	505, 238, 2.1, 0.1
Venezuela	1257, 263, 4.8	2769, 418, 6.6	1842, 375, 4.9	118, 52, 2.3	79, 36, 2.2	8, 8, 1.0	27, 20, 1.4	4, 3, 1.3	49, 34, 1.4	18, 16, 1.1	27, 20, 1.4	434, 147, 3.0	6554, 1066, 6.1, 0.7
Vietnam	27, 8, 3.3	191, 46, 4.2	93, 23, 4.1	25, 12, 2.1	0, 0, 0	-	-	-	10, 1, 10.1	0, 0, 0	18, 7, 2.6	9, 3, 2.9	367, 85, 4.3, 0.1
Yemen	2, 2, 1.0	9, 5, 1.7	2, 2, 1.0	0, 0, 0	4, 3, 1.3	-	-	-	0, 0, 0	0, 0, 0	2, 2, 1.0	1, 1, 1.0	19, 13, 1.5, 0
Yugoslavia (former)	-	-	-	81, 39, 2.1	30, 9, 3.3	9, 8, 1.1	68, 26, 2.6	278, 85, 3.3	383, 139, 2.8	499, 237, 2.1	-	-	1348, 505, 2.7, 0.5
Zambia	-	-	-	1429, 248, 5.8	2146, 271, 7.9	14125, 2031, 7.0	30584, 3784, 8.1	16040, 2679, 6.0	33239, 5382, 6.2	12114, 2111, 5.7	596, 261, 2.3	88, 28, 3.1	110285, 13049, 8.5, 14.7
Zimbabwe	-	-	-	157, 59, 2.7	65, 32, 2.0	107, 50, 2.1	1046, 226, 4.6	2551, 418, 6.1	7865, 1761, 4.5	4846, 697, 7.0	854, 245, 3.5	23, 17, 1.3	17513, 3013, 5.8, 4.5

Burned areas statistics reported at country level for the year 2000. Number of burn scars, average scar size and % of each country burned in the year 2000 are shown.

political boundary map as given in Table II. The column on the far right in Table II describes the results of the annual synthesis. Topping the table of total burned area per country in the year 2000 is Australia with 558,867 km² that accounts for 7.3% of the total surface area of Australia with an average burned scar size of 28.4 km². Three African countries, Sudan (403,099 km²), Angola (296,545 km²) and DR Congo (260,032 km²) follow Australia. Average scar size in these countries range between 14.6 km² and 22.6 km². The total burned area in Russia was estimated at 223,575 km². However, what is interesting about the results for Russia (and also for Kazakhstan) is that the average scar size, estimated at 3.4 km² and 4.6 km² respectively, is much smaller than is the case for many African nations and Australia. Also the total number of burn scars in Russia was very high with over 66,000 individual scars being detected compared to between 7,500 and 23,000 for the other countries in the top 15 list. In the Central African Republic the number of individual burn scars detected is low compared to surrounding countries (7,592 scars). However, the average size of a burn scar is second only to Australia at 24.4 km² resulting in a total burned area of 185,479 km². After Russia, the next five countries with burned areas sorted into descending order are African nations (Central African Republic, Ethiopia, Tanzania, Zambia and Mozambique). For the western hemisphere countries, Argentina recorded the highest total burned area with an average scar size of 3.3 km² and quite a large number of individual scars detected (16,717 scars). The United States followed with an estimated 34,963 km² of burned areas, affecting approximately 0.4% of the total surface area of the country. Of particular interest is that the estimated burned area for Brazil (18,293 km²) in the year 2000, came after the two countries named above and also Mexico (21,226 km²). In addition, the annual estimate for Canada is 5,687 km² that is much lower than the 1989–1998 ten-year average of 33,580 km² (Fraser et al., 2003). A discussion of the validity and relevance of these estimates and reasons for their derivation is presented later in this paper. The countries in which vegetation burning has the greatest influence on the land cover and has the largest impact on the people who live there can be estimated by looking at the percentage of the total surface area of the country that has been burned. Here we see that the table is dominated by the African nations, occupying the top 15 places. At the top is the Central African Republic where 30% of the land surface is affected by burning, in position 15 is The Gambia where 7.6% of the surface is burned.

The estimated global burned area for the year 2000 is just over 3.5 million km². Because of different burning seasons the actual amount of biomass consumed by fire is higher than is reflected in the annual burned area total, because some regions (those located in the tropical Northern Hemisphere) were burned twice in the year 2000. On a monthly basis, it was during the month of December 2000 that the greatest burned areas were detected comprising 523,496 km² or 14.9% of the total annual burned area. Combined with the area estimated in January 2000, 438,715 km² over 25% of the total annual burned area occurs during these two months. This peak in burning activity is associated with burning in the Northern Hemisphere

sub-tropical belt as well as in temperate regions of the Southern Hemisphere. Another peak in activity, together accounting for 40% of global burned areas, occurs in the months of June (9% of the global burned area), July (10.6%), August (9.6%) and September (10.9%) that corresponds to burning activity in the temperate and boreal zones in the Northern Hemisphere and also burning in the Southern Hemisphere sub-tropical belt and in Australia.

4.2. A MONTH BY MONTH DESCRIPTION OF BURNING ACTIVITY IN THE YEAR 2000

In this section, all reported estimates of burnt areas (normally shown in brackets) are in square kilometers (km²). In January 2000, significant burning activity is detected in the sub-Saharan region of Africa, concentrated in southern Sudan (140,950), Central African Republic (95,668), Ghana (9,776), Chad (13,457), Ethiopia (29,344), Kenya (9,745), northern Democratic Republic of the (DR) Congo (15,288), Nigeria (7,499) and northern Uganda (19,946). Burning activity is detected in the grassland area of the Llanos of the Orinoco in Venezuela (1,257) and Colombia (2,068), the Pampas of central and southern Argentina (3,168) and, to a lesser extent in Chile (348). Activity is also detected in Mexico (2,967) and southern states of the US (688), the southern Indian peninsula (3,917), southern China located north of Vietnam (3,084), Burma (2191) and in Cambodia (755). Burning is widespread in Australia (except for the tropical regions in the north) mainly down the east and western flanks (45,263).

February 2000 sees a reduction in burning activity in the sub-Saharan Africa region. The activity has shifted southwards slightly but there are large regions of burning activity remaining along the Sudan (42,871) and Ethiopian (19,906) border. Burning activity is still on-going in the grassland regions of Venezuela (2,769), Colombia (4,524), northern Brazil (566) and increasing in Mexico (3,193). Activity is increasing in Cambodia (3,006) and southern China (4,335). Activity in Australia remains high with concentrations of activity detected in the non-tropical northwest and west (27,515).

March 2000 sees, once again, a large number of burned scar detections in Australia (16,924). The activity in India (12,937) peaks in March of the year 2000, whereas the activity has almost ceased in Thailand (118), Vietnam (93) and Laos (80). Activity in southern China (6,324) is increasing in area and becoming more widespread. In sub-Saharan Africa activity is beginning to cease, with the onset of the wet season in May. However, some late season burning is still occurring, namely in the southern Sudan (23,072) and Ethiopia (22,160). In Central America, burning is still detected in Mexico (1,864) however, now the burned scars are slightly larger and less numerous. Burning is on-going in the Llanos of the Orinoco covering both Venezuela (1,842) Colombia (2,905), and also in central Argentina (2,468). The burned areas detected during the months of January through to March 2000 are shown in blue in Figure 1 (bottom).

April is associated with the end of the Northern Hemisphere winter and the onset of the Southern Hemisphere winter and consequent dry season. Burning activity that can be described as being both widespread and intense is observed in the region of southwest Russia (the total for Russia is 99,927), eastern Ukraine (14,980) and northern Kazakhstan (37,811) associated with agricultural land use in the region. It is thought to be due to early season agricultural waste burning and further evidence is seen on quick-look Landsat TM scenes. Burn scars are, in fact, detected all along this belt of steppe grassland and agriculture at around 50°N (apart from desert and mountain areas) to eastern Mongolia (7,597), southern Russia, North Korea (1,057) and northern China (total for China is 19,084). Late season burning is still occurring in India (9,549) and peaks in Burma (4,241) although the monsoon period is now only a few months away. April is the month of least burning activity in Australia (10,740). Burning activity is now diminishing rapidly in sub-Saharan Africa during April. Fires occurring at these times, mainly in Ethiopia (11,470) and Sudan (10,012), are really at the end of the dry season. The zone of fire activity has now shifted to the south with activity starting to pick up in Kenya (3,226). The least amount of activity in the year 2000 is detected in the DR Congo during April (295). The beginnings of the Southern Hemisphere fire season seen in northern Angola (2,670), northern Zambia (1,429) and in the borderlands of Lesotho (337). In South America, burning activity has all but ceased. Very few burn scars are being detected in the Llanos of the Orinoco, and progressing further north, detections are now restricted to the south of Mexico (1,861) and also in Cuba (190). In North America (north of 30°N), April is the onset of summer, the main season of burning activity. However, detections made during April (3,512 for the US and 20 for Canada) are restricted to mainly agricultural regions, the main one being located in the States of Kansas and Oklahoma.

During May 2000, no significant detections are made in Canada (24). In the US (1,840) activity is located mainly in northern California. Burning in Mexico (2,378) continues even into May indicating that the rains have not yet commenced. Burning activity is now detected in the coastal regions of Peru (1,944) and also in Bolivia (787), now that the Southern Hemisphere dry season has started. Activity is now quite widespread and intense throughout Argentina (8,807) and Chile (421) between 28 and 38°S. Burning activity is extremely intense in southern DR Congo (26,225), northern Angola (4,994), Kenya (7,283) and western Tanzania (5,969). Activity is still detected in southern Sudan (11,276) and Ethiopia (6,288). Further south, burn scar detections are observed in Namibia (4,771), South Africa (2,542) and first observations are seen in southwest Madagascar (433). North of the Sahara, activity is detected at the delta of the Nile in Egypt (812). In May 2000, activity in western Europe was almost non-existent. Further east, activity is detected in eastern Ukraine (1,554), parts of Turkey (486), southern Russia (especially in the delta region of the Volga River), and again at the border between Russia (total for Russia is 75,820) and Kazakhstan (6,668) but with less extent than in April. Isolated scars are detected now further north in Russia. Burning activity in the region of

eastern Mongolia (13,688), southeastern Russia (as reported above) and northern China (9,632) is now extremely intense. Extremely large and continuous burn scars are observed in these areas. Burning activity has ceased in continental, southeast Asia but continues in India (8,917) just before the monsoon starts. In Australia (13,995), May is the beginning of the dry season in the north of the country and already large burn scars are being detected in this region and also in the east of the country.

In June 2000, detection of activity in Australia is increasing (22,582) in the states of the Northern Territory and northern Western Australia. Activity has ceased in India and southern China and has diminished and become isolated in northern China (total for China is 6,449), Mongolia (2,845) and the Steppe regions of southern Russia. Activity in Russia (total for Russia is 16,005) is observed now in forested areas with the onset of hot, dry and stable weather. Activity at the border between Russia and Kazakhstan (6,192) has reduced by a considerable amount. A considerable amount of activity is detected in central and southern Italy, Sicily, Sardinia (total for Italy is 1,289), Spain (331) and Portugal (91). The situation in Africa is that burning has but almost ceased north of the equator and has become incredibly intense and widespread throughout northern Angola (70,341), southern DR Congo (90,478), western Tanzania (35,267) and Zambia (14,125). Burn scars are also detected in the southwest corner of Botswana (10,106) and in South Africa (17,120). In Madagascar, burning activity is restricted to the dryer western half of the island (1,592). To the west across the Atlantic, burning activity is still continuing in central parts of northern Argentina (4,157) and is beginning in southern and eastern regions of Brazil (1,721), specifically in the Mato Grosso and Goias districts, as well as in parts of Bolivia (360). Burn scars are detected in the western states of the US (1,607) in June 2000, but not on a large scale. The first detections are observed in Canada (254) and Alaska (included in the figure given above for the US). In Figure 1 (bottom), burned area detections made between April and June 2000 are shown in red.

In July 2000, burning activity in the forests of Canada (1,355) and Alaska (included in the figure for the US given below) and in the western states of the US (total for the US including Alaska is 4,917) are detected. In central and southern Brazil (2,910), Bolivia (2,196) and northern Argentina (7,653) burning activity is increasing, but not at the scale seen in southern Africa. In Angola (112,482), almost all of the country is being affected by burning activity. The intensity of activity is also being maintained in southern DR Congo (87,739), Zambia (30,584) and eastern and southern Tanzania (29,900). As well as moving south, the burning activity is also slowly progressing east. Large burn scars are now being detected in Mozambique (15,818) and eastern South Africa (9,516). In Zimbabwe there appears to be very little burning activity detected during the Southern Hemisphere dry season. The peak month of activity is detected in September (7,865) but compared with countries surrounding Zimbabwe, the area burned is much smaller. In Madagascar (1,178) the burning activity is progressing further east. Burn scars are detected in Morocco

(375), Portugal (46), Spain (151) and southern Italy (108). Activity is detected in southern Russia (the total for Russia is 7,897), near the border with Georgia and in central Kazakhstan (4,248), northwest China (1,867) and southeast Russia (included in the total given above). Burn scars detected in Siberian forests are quite large and isolated. Isolated, small burn scars are detected on several islands in Indonesia (77) and Malaysia (26). Activity in Australia (28,167) is detected in Cape York, Northern Territory and northern and central parts of Western Australia.

August 2000 sees an increase in burning activity in Australia (69,616), especially in the north, but also in the southwest of the country. Detections are made in the Indonesian islands (513). In eastern Siberia (the total for Russia is 14,432), burning activity is restricted to mainly forest fires that are quite large in size, but isolated. Large burn scars are observed in central Kazakhstan (16,836) and also further south in Kyrgyzstan (828) and Tajikistan (285) and in countries surrounding the Black Sea including Russia, Ukraine (2,575) and Bulgaria (763). Burning activity in western Europe peaks in Portugal (369) and remains high in Spain (321) during August 2000 and is observed in northern Algeria (377), southern Italy (191) and Greece (186). In southern Africa, the main region of burning activity is moving south and east, but still remains intense throughout Angola (66,005), Zambia (16,040), Kenya (6,701), Tanzania (17,673), South Africa (10,109), Namibia (3,997) and Malawi (699). In Mozambique (32,812), burning activity is very intense and activity is still increasing in Madagascar (1,775). Across the Atlantic, activity is increasing in central and southern Brazil (7,400) and in Paraguay (270). In North America, burn scars are continuing to be detected in western US including Alaska (5,066) and Canada (2,824).

In September 2000, the peak of the burning activity in North America is observed. Extensive burned areas are detected in the forest and woodland regions of Montana, Idaho, Wyoming, Colorado, North Dakota and Minnesota (total for the US including Alaska is 14,790). The peak month of burning activity in Canada occurred in August, with September's value being much lower (1,207). September 2000 also saw a diminishing of the burning activity in central and southern Brazil (2,500) and an increase of activity detected in northern Bolivia (3,516) and northern Argentina (5,559). The dry season in southern Africa is still very much in place and the main region of burning activity still pushes further south and east. Activity in the west of southern Africa is located in the coastal regions of Angola (33,158) and further south in Botswana (6,003) and Namibia (12,745). Activity is detected all along the eastern edge of southern Africa, from South Africa (19,752), through Mozambique (32,074), Zambia (33,239) and Tanzania (12,466) to Kenya (13,903) and Somalia (6,024). Activity peaks in Algeria (883) and Spain (564) and continues in Italy (565), Greece (71) and Portugal (211) throughout September. Some burn scars are detected in eastern European countries such as Hungary (640) and Romania (770), southern Russia (the total for Russia is 3,186) and Kazakhstan (8,546) that could be due to the burning of agricultural land. In September 2000, the peak in burning activity is detected in the Indonesian islands (the total for all

islands is 916), the same being true for Papua New Guinea (96). The peak of burning activity in Australia is observed in September 2000 (140,393). In Figure 1 (bottom), burn scars detected between July and September are shown in green.

The month of October 2000 is normally characterized by the onset of the dry season (winter period) in the Northern Hemisphere tropical belt, associated with the commencement of burning activities in the northern tropics and diminishing of activities in the southern tropics. In Australia, we are seeing more activity in the center and south of the country (84,243). Detections are made in India (3,179), Nepal (957) and on the Tibetan Plateau in China (the total for China is 6,348). In the northeast of China, activity has again increased possibly due to agricultural waste burning or land clearance. Activity is detected in Russia (6,309), concentrated in the border region with Kazakhstan (1,321) and also in North Korea (693). In sub-Saharan Africa, burning activity starts during October 2000 in southern Mauritania (8,515), Mali (3,747), northeast Nigeria (3,235), central Chad (19,484) and in regions of Sudan (12,433) and Ethiopia (4,124) in a line running at approximately 15°N of the equator. In southern Africa, the burning activity is generally diminishing. However, regions of intense burning activity are still observed in central Botswana (11,865), Zambia (12,114) and northern Mozambique (19,765). Activity in Madagascar (1,899) is now situated in towards the eastern side of the island. A reduction in burning activity is seen in northern Argentina (1,574), southern Brazil (2,294) and Bolivia (685). No activity is detected in October in the Llanos of the Orinoco. Burning activity has commenced in Mexico (1,876) and has practically ceased in North America.

In November 2000, burn scars are detected in Mexico (4,082) as the early dry season progresses. In southern Argentina, at the beginning of the Southern Hemisphere summer, activity is being detected. In southern Africa the fire season is ending fast with the onset of the wet season, a concentration of burning activity is still observed in the southwest corner of South Africa (7,824) and northern Madagascar (1,062). Burning activity north of the equator in Africa is really starting to dominate the landscape with detections made in Senegal (3,324), Mali (8,608), Ghana (4,398), Benin (1,769), northern Cameroon (6,676), southern Chad (18,046), northern Central African Republic (11,216), Ethiopia (8,765) and all across southern Sudan (63,246). Further east, burning activity is detected in isolated regions across central India (2,922) and in southern China (1,561) and Laos (411). Burning is still occurring at a very large scale in Australia (85,698), dominant in the State of Queensland.

In December 2000, burning activity in Australia (13,732) diminishes as rains come to the north of the country but still occurring on a smaller scale in the State of Western Australia. In Africa, north of the equator, burning activity is increasing rapidly, slowly pushing further south and now dominant in a belt between 5 and 14°N (with the exception of Sierra Leone, Liberia and parts of Somalia) and including Sudan (169,385), Ghana (42,073), Benin (9,943), Chad (23,950), Cameroon (33,316), the Central African Republic (99,095), Somalia (6,753), Togo (5,407),

Nigeria (11,399) and the Ivory Coast (18,615) that peak in December, Senegal (1,957), Mali (3,134), Ethiopia (29,341). In South America, burning activity is detected in Argentina (6,696) at approximately 36°S and we observe the beginnings of burning activity in the Llanos of the Orinoco in Venezuela (434) and Colombia (98). In Mexico (3,964), burning activity is observed with a large number of burn scars detected that are relatively small in area. Some burning is also detected in the State of Florida in the US (518). In Figure 1 (bottom), burn scars detected between October and December are shown in yellow-orange.

4.3. THE YEAR 2000 INVENTORY AS A REFERENCE DATASET

It has been shown in the literature that there is significant multi-annual variation in the spatial distribution and also in the timing of vegetation fires. The causes of these fluctuations are mainly driven by climatic factors such as temperature, precipitation and humidity. They may also be caused by changes in the management or use of the land. In the boreal regions, the inter-annual variation in burned area can be very large indeed. It was well documented in the world's media that in the summer of 1998, huge regions of forests were lost in Russia and Canada. In the literature, devastating fires in Siberia, Mongolia and northern China during 1987 (Cahoon et al., 1994) have been described. Large scale climatic phenomena, such as El Niño and La Niña that are disruptions of the ocean-atmosphere system in the tropical Pacific Ocean, can have a large impact on the severity and distribution of vegetation burning at a global scale. The 1997 El Niño year, characterised by a long dry season and elevated temperatures in the west Pacific resulted in devastating fires in Indonesia (Siegart et al., 2001) resulting in a huge release of carbon (0.81–2.57 gigatonnes) to the atmosphere (Page et al., 2002). The year 2000 was a La Niña year characterised by unusually cool temperatures in the equatorial Pacific Ocean. This may be the reason why we observe a mild fire season in Brazil and Indonesia and a severe fire season in the United States. The large inter-annual variability of carbon emissions caused by biomass burning between 1997 and 2001 has also been demonstrated by Van der Werf et al. (2004), who revealed that negative global carbon monoxide anomalies occurred in the year 2000. To further highlight the potential annual variability in burning activity, the frequency of active fires detected by the ATSR-2 satellite acquired at night-time for the period 1997 to 2000 have been calculated. The numbers of fires detected were 133,970 (1997), 178,547 (1998), 120,650 (1999) and 116,478 (2000). These data show that in the year 2000, the least number of fires were detected. It could therefore be assumed that the results presented in this paper reflect a lower than average estimate of burnt areas. The authors state that the burned area estimates should be used with caution if the user intends to describe general conditions or make extrapolations for other years. Multi-annual estimates using the same techniques are required for several years including years experiencing several El Niño and La Niña events.

4.4. VALIDATION ISSUES AND ERRORS IN THE GBA, 2000 INVENTORY

A global validation of the GBA, 2000 product is not available at this time. Neither is a figure for the overall accuracy of the burned area map at the global scale. Work is currently being undertaken to derive a benchmark dataset for the validation of global scale thematic maps of biomass burning. The work is foreseen to be completed by the end of 2004 and will be published in refereed journals. Preliminary results have been presented at the recent CEOS Calibration/Validation Landcover Products Workshop in Boston and further work will be made presented at the 20th International Society for Photogrammetry and Remote Sensing Conference in Turkey in July 2004. For each of the regional algorithms a performance indicator is available, derived using selected Landsat TM scenes over the corresponding region of interest. An outline of the performance of the algorithms is given in Grégoire et al. (2003).

It is useful to indicate to the reader, regions where the authors believe there may be some errors in the GBA, 2000 product, through either false detection's or burned areas that are not detected. Throughout the implementation of the regional burned area algorithms, care was taken to ensure that no large errors of commission or omission were made. These checks were made using quick-look Landsat TM imagery available freely over the Internet, evidence of burning activity in the VGT products such as smoke and fire fronts, and evidence of burning activity documented in the media. It is important to note that when the regional products were joined together, no major artifacts were observed at the join between regions. Artificial edge effects, however, are observed in central, southern Russia near to the Kazakhstan border. The artifacts are caused by the inherent properties of the IFI algorithm that calculates the burned areas over a 200 km by 200 km window. An in-depth investigation was made to understand the occurrence of these artifacts and they are believed to be caused by contamination of the image data (e.g. fire smoke, raw data processing) that is not masked out during the various data cleaning processes applied to the data. These artifacts are only observed in the region of southern Russia and, given that the IFI algorithm is used extensively elsewhere with no further occurrences reported, it was decided to accept these artifacts in the final product.

It is understood that there is a small underestimation of burned areas in Canadian forests and a commission error from falsely mapped fires of approximately 20% (Fraser et al., 2003). In the US, there may be some false detections in the semi-arid regions but this has not been confirmed. In parts of Mexico, due to complex land surface properties, cloud cover and small burned areas, it is difficult to evaluate the algorithms performance. For the whole of Central America, due to the same factors mentioned above, the true burned area has probably been underestimated. In Brazil, we understand that we are not detecting smaller burned areas and burning beneath the forest canopy. In addition, due to strong phenological influences in the east of Brazil, we believe that an underestimation of the true burned area is made. Significant areas of shadow caused by topography from the Andes mountain range may yield some false detections. Estimation of the true burned area in Europe

and northern Africa provides difficulties because of the often-small size of the fire events and burn scar. It is believed, though it has not been proven, that over half of the land area in a pixel needs to burn before being detected by the algorithms, although this may depend on the algorithm being used. In the sub-Saharan region of Africa, small errors are present in the burned area products, these are mainly caused by flooding of non-permanent water features and dark rocks in the east of Africa. Compared with the magnitude of burning in Africa, these false detections are insignificant. In southern Africa, fire occurrence at the start of the rainy season may have been missed due to cloud cover. In central and eastern Russia and northern Asia, it is understood that there are small areas of falsely detected burn scars in forested ecosystems and a small amount of omitted pixels in grassland ecosystems. A number of burned areas in insular southeast Asia are not detected, caused mainly by excessive cloud coverage, a limited number of good observations of the ground surface and, in common with the Amazon, many of burned areas being too small to detect. In Australia, it is understood that the GBA, 2000 product underestimates the true burnt area. However, certain types of burning activity in Australia, for example occurring in sparse, hummock *Spinifex* grasslands growing in bright, red sand soils (Graetz, personal communication, 2002) cause the surface to increase in reflectance. The GBA, 2000 algorithms mainly look for a drop in reflectance.

5. Conclusions

An inventory of the extent of burned vegetation for the year 2000 is described in this paper, with reference to the seasonality and timing of burning activity on a monthly basis and tabulated estimates of burned areas per country at global extent. The global burned area products are available to the user community, free of charge through the Internet at the following website (<http://www.gvm.jrc.it/fire/gba2000/index.htm>). An accuracy assessment of the GBA, 2000 product is currently underway. The methodology developed by the GBA, 2000 initiative will be used in the implementation of the GlobCarbon project of the European Space Agency, providing global, monthly, burned area products over 5 years (1999–2003) from SPOT VGT data.

References

- Andreae, M. O. and Merlet, P.: 2001, 'Emission of trace gases and aerosols from biomass burning', *Global Biogeochem. Cycles* **15**, 955–966.
- Barbosa, P. M., Grégoire, J.-M., and Pereira, J. M. C.: 1999a, 'An algorithm for extracting burned areas from time series of AVHRR GAC data applied at a continental scale', *Remote Sensing Environ.* **69**, 253–263.
- Barbosa, P. M., Stroppiana, D., Grégoire, J.-M., and Pereira, J. M. C.: 1999b, 'An assessment of vegetation fire in Africa (1981–1991): Burned areas, burned biomass, and atmospheric emissions', *Global Biogeochem. Cycles* **13**, 933–950.
- Boschetti, L., Flasse, S., Trigg, S., and de Dixmude, A. J.: 2002, 'A multitemporal change detection algorithm for the monitoring of burnt areas with spot vegetation data', in Bruzzone, L. and Smits,

- P. (eds.), *Analysis of MultiTemporal Remote Sensing Images*, World Scientific, Singapore, pp. 75–82.
- Breiman, L., Friedman, J. H., Olshen, R. A., and Stone, C. J.: 1984, *Classification and Regression Trees*, Wadsworth & Brooks, California.
- Brivio, P. A., Maggi, M., Binaghi, E., Gallo, I., and Grégoire, J.-M.: 2002, 'Exploiting spatial and temporal information for extracting burned areas from time series of SPOT-VGT data', in Bruzzone, L. and Smits, P. (eds.), *Analysis of MultiTemporal Remote Sensing Images*, World Scientific, Singapore, pp. 132–139.
- Cahoon Jr., D. R., Stocks, B. J., Levine, J. S., Cofer III, W. R., and Pierson, J. M.: 1994, 'Satellite analysis of the severe 1987 forest fires in northern China and southeastern Siberia', *J. Geophys. Res.* **99**, 627–638.
- Colby, J. D.: 1991, 'Topographic normalization in rugged terrain', *Photogramm. Eng. Remote Sensing* **57**, 531–537.
- Conard, S. G., Sukhinin, A. I., Stocks, B. J., Cahoon, D. R., Davidenko, E. P., and Ivanova, G. A.: 2002, 'Determining effects of area burned and fire severity on carbon cycling and emissions in Siberia', *Climate Change* **55**, 197–211.
- Dwyer, E., Pereira, J. M. C., Grégoire, J.-M., and DaCamara, C. C.: 1999, 'Characterization of the spatio-temporal patterns of global fire activity using satellite imagery for the period April 1992 to March 1993', *J. Biogeogr.* **27**, 57–69.
- Eastwood, J. A., Plummer, S. E., Wyatt, B. K., and Stocks, B. J.: 1998, 'The potential of SPOT-vegetation data for fire scar detection in boreal forests', *Int. J. Remote Sensing* **19**, 3,681–3,687.
- Ershov, D. V. and Novik, V. P.: 2001, 'Mapping burned areas in Russia with SPOT4 VEGETATION (S1 Product) imagery', Final Report for the Joint Research Centre of the European Commission, contract number: 18176-2001-07-F1EI ISP RU.
- Eva, H. D., Malingreau, J. P., Grégoire, J.-M., Belward, A. S., and Mutlow, C. T.: 1998, 'The advance of burnt areas in Central Africa as detected by ERS-1 ATSR-1', *Int. J. Remote Sensing* **19**, 1,635–1,637.
- Fernández, A., Illera, P., and Casanova, J. L.: 1997, 'Automatic mapping of surfaces affected by forest fires in Spain using AVHRR NDVI composite data', *Remote Sensing Environ.* **60**, 153–162.
- Fraser, R. H., Fernandes, R., and Latifovic, R.: 2003, 'Multi-temporal mapping of burned forest over Canada using satellite-based change metrics', *Geocarto Int.* **18**, 37–48.
- Fraser, R. H., Li, Z., and Cihlar, J.: 2000, 'Hotspot and NDVI differencing synergy (HANDS): A new technique for burned area mapping over boreal forest', *Remote Sensing Environ.* **74**, 362–376.
- Grégoire, J.-M., Tansey, K., and Silva, J. M. N.: 2003, 'The GBA, 2000 initiative: Developing a global burned area database from SPOT-VEGETATION imagery', *Int. J. Remote Sensing* **24**, 1,369–1,376.
- Hansen, M. C., Defries, R. S., Townshend, J. R. G., and Sohlberg, R.: 2000, 'Global land cover classification at 1 km spatial resolution using a classification tree approach', *Int. J. Remote Sensing* **21**, 1,331–1,364.
- Hastings, D. A. and Dunbar, P. K.: 1998, 'Development and assessment of the global land one-km base elevation digital elevation model (GLOBE)', *Int. Soc. Photogramm. Remote Sensing Arch.* **32**, 218–221.
- Houghton, R. A.: 1991, 'Biomass burning from the perspective of the global carbon cycle', in Levine, J. S. (ed.), *Global Biomass Burning: Atmospheric, Climatic, and Biospheric Implications*, MIT Press, Cambridge, MA, pp. 321–325.
- Isaev, A. S., Korovin, G. N., Bartalev, S. A., Ershov, D. V., Janetos, A., Kasischke, E. S., Shugart, H. H., French, N. H. F., Orlick, B. E., and Murphy, T. L.: 2002, 'Using remote sensing to assess Russian forest fire carbon emissions', *Climate Change* **55**, 235–249.
- Johnson, R. A. and Wichern, D. W.: 1988, *Applied Multivariate Statistical Analysis (Second Edition)*, Prentice Hall, New Jersey.

- Kasischke, E. S., Christensen, N. L., and Stock, B. J.: 1995, 'Fire, global warming, and the carbon balance of boreal forests', *Ecol. Appl.* **5**, 437–451.
- Kempeneers, P., Swinnen, E., and Fierens, F.: 2002, GLOBSCAR Final Report, TAP/N7904/FF/FR-001 Version 1.2, VITO, Belgium.
- Levine, J. S.: 1996, 'FireSat and the global monitoring of biomass burning', in Levine, J. S. (ed.), *Biomass Burning and Global Change*, The MIT Press, Cambridge, MA, pp. 107–132.
- Malingreau, J. P. and Grégoire, J.-M.: 1996, 'Developing a global vegetation fire monitoring system for global change studies: A framework', in Levine, J. S. (ed.), *Biomass Burning and Global Change*, The MIT Press, Cambridge, MA, pp. 14–24.
- Page, S. E., Siegart, F., Rieley, J. O., Boehm, H.-D. V., Jaya, A., and Limin, S.: 2002, 'The amount of carbon released from peat and forest fires in Indonesia during 1997', *Nature* **420**, 61–65.
- Pereira, J. M. C.: 1999, 'A comparative evaluation of NOAA/AVHRR vegetation indices for burned surface detection and mapping', *IEEE Trans. Geosci. Remote Sensing* **37**, 217–226.
- Pereira, J. M. C., Mota, B. W., Privette, J. L., Caylor, K. K., Silva, J. M. N., Sá, A. C. L., and Ni-Meister, W.: in press, 'A simulation analysis of the detectability of understory burns in Miombo Woodland', *Remote Sensing Environ.*
- Pereira, J. M. C., Pereira, B. S., Barbosa, P. M., Stroppiana, D., Vasconcelos, M. J. P., and Grégoire, J.-M.: 1999, 'Satellite monitoring of fire in the EXPRESSO study area during the 1996 dry season experiment: Active fires, burnt area and atmospheric emissions', *J. Geophys. Res.* **104**, 30,701–30,712.
- Roujean, J. L., Leroy, M., and Deschamps, P. Y.: 1992, 'A bi-directional reflectance model of the earth's surface for the correction of remotely sensed data', *J. Geophys. Res.* **97**, 20,455–20,468.
- Roy, D., Lewis, P. E., and Justice, C. O.: 2002, 'Burned area mapping using multi-temporal moderate spatial resolution data—A bi-directional reflectance model-based expectation approach', *Remote Sensing Environ.* **83**, 263–286.
- Scholes, R. J., Kendall, J., and Justice, C. O.: 1996, 'The quantity of biomass burned in Southern Africa', *J. Geophys. Res.* **101**, 23,667–23,676.
- Schultz, M. G.: 2002, 'On the use of ATSR fire count data to estimate the seasonal and interannual variability of fire emissions', *Atmos. Chem. Phys. Discuss.* **2**, 1,159–1,179.
- Siegart, F., Ruecker, G., Hinrichs, A., and Hoffmann, A. A.: 2001, 'Increased damage from fires in logged forests during droughts caused by El Nino', *Nature* **414**, 437–440.
- Silva, J. M. N., Pereira, J. M. C., Cabral, A. I., Sá, A. C. L., Vasconcelos, M. J. P., Mota, B., and Grégoire, J.-M.: 2003, 'The area burned in Southern Africa during the 2000 dry season', *J. Geophys. Res.* **108**, D13, 8498, doi: 10.1029/2002JD002320.
- Silva, J. M. N., Sousa, A. M. O., Pereira, J. M. C., Tansey, K., and Grégoire, J.-M.: 2002, 'A Contribution for a Global Burned Area Map', in Viegas, D. X. (ed.), *Forest Fire Research & Wildland Fire Safety*, Millpress, Rotterdam.
- Stroppiana, D., Pinnock, S., Pereira, J. M. C., and Grégoire, J. M.: 2002, 'Radiometric analysis of spot vegetation images for burnt area detection in Northern Australia', *Remote Sensing Environ.* **82**, 21–37.
- Stroppiana, D., Tansey, K., Grégoire, J.-M., and Pereira, J. M. C.: 2003, 'An algorithm for mapping burnt areas in Australia using SPOT-VEGETATION data', *IEEE Trans. Geosci. Remote Sensing* **41**, 907–909, doi: 10.1109/TGRS.2003.808898.
- Tansey, K.: 2002, *Implementation of the Regional Burnt Area Algorithms for the GBA, 2000 Initiative*, Publication of the European Communities, EUR 20532 EN.
- Tansey, K., Grégoire, J. M., Stroppiana, S., Sousa, A., Silva, J. M. N., Pereira, J. M. C., Boschetti, L., Maggi, M., Brivio, P. A., Fraser, R., Flasse, S., Ershov, D., Binaghi, E., Graetz, D., and Peduzzi, P.: 2004, 'Vegetation burning in the year 2000: Global burned area estimates from SPOT VEGETATION data', *J. Geophys. Res.* **109**, D14503 doi: 10.1029/2003JD003598.

- Trigg, S. and Flasse, S.: 2000, 'Characterizing the spectral-temporal response of burned savannah using in situ spectroradiometry and infrared thermometry', *Int. J. Remote Sensing* **21**, 3,161–3,168.
- Van Aardenne, J. A., Dentener, F. J., Olivier, J. G. J., Klein Goldewijk, C. G. M., and Lelieveld, J.: 2001, 'A $1^\circ \times 1^\circ$ resolution data set of historical anthropogenic trace gas emissions for the period 1890–1990', *Global Biogeochem. Cycles* **15**, 909–928.
- Van der Werf, G. R., Randerson, J. T., Collatz, G. J., Giglio, L., Kasibhatla, P. S., Avelino, A., Olsen, S. C., and Kasischke, E. S.: 2004, 'Continental-scale partitioning of fire emissions during the 1997–2001 El Niño/La Niña period', *Science* **303**, 73–76.
- Wotawa, G., Novelli, P. C., Trainer, M., and Granier, C.: 2001, 'Inter-annual variability of summertime CO concentrations in the Northern Hemisphere explained by boreal forest fires in North America and Russia', *Geophys. Res. Lett.* **28**, 4,575–4,578.

(Received 13 May 2003; in revised form 14 June 2004)